Submitted in accordance with the requirements for the degree of
Doctor of Philosophy

UNIVERSITY OF LEEDS

SCHOOL OF PHYSICS & ASTRONOMY

Dissecting Topological Quantum Computation

James Robin Wootton

May 2010

Work which has formed part of jointly authored publications has been included in this thesis. I, the candidate, am the lead author of each of these, with the other authors primarly contributing through advice and supervision. All work presented in this thesis is directly attributable to myself.

The chapters including jointly authored work are: Chapter 3, based upon [1] done in collaboration with Jiannis K. Pachos; Chapter 4, based upon [2] done in collaboration with Ville Lahtinen, Zhenghan Wang and Jiannis K. Pachos; and Chapter 5, based upon both [3] and [4], both done in collaboration with Ville Lahtinen and Jiannis K. Pachos, with the latter also involving Benoit Doucot. Elements of [4] are also present in Chapter 6.

Acknowledgements

Thanks be to God, without whose pioneering work in the creation of the universe, none of this would be possible. Thanks also to my parents for causing me to exist, allowing me to have a shed and supporting me through my studies. Thanks to my wife, for listening to the incomprehensible rants caused by my PhD studies, and to my sister for being my sister. Any other family members who feel they ought to be thanked are also duly thanked for all that they did.

Thanks to Dr. Jiannis K. Pachos for his supervision during my PhD, and to Ville Lahtinen for collaborations both in the office and in the pub. Thanks also to Jonathan Busch for conversations on nautical philosophy, to Abbas Al Shimary for reminding when it is time for tea on those rare occasions that I forget, and to my fellow Erosians for helping me escape Leeds every now and again, and enjoy the hospitality of a more civilised city. All those involved in making Star Trek also deserve my eternal gratitude for the continual inspiration they have brought me.

I began these acknowledgements by thanking God. I will end by thanking something almost as divine. Thanks be to tea, the nectar without which this thesis could never have been completed.

Abstract

James Robin Wootton, "Dissecting Topological Quantum Computation", Ph.D. thesis, University of Leeds, May 2010.

Anyons are quasiparticles that may be realized in two dimensional systems. They come in two types, the simpler Abelian anyons and the more complex non-Abelian anyons. Both of these have been considered as a means for quantum computation, but non-Abelian anyons are usually assumed to be better suited to the task. Here we challenge this view, demonstrating that Abelian anyon models have as much potential as some simple non-Abelian models.

First the means to perform quantum computation with Abelian anyon models is considered. These models, like many non-Abelian models, cannot realize universal quantum computation by braiding alone. Non-topological operations must be used in addition, whose complexity depends on the physical means by which the anyons are realized. Here we consider anyons based on spin lattice models, with single spin measurements playing the role of non-topological operations. The computational power achieved by various kinds of measurement is explored and the requirements for universality are determined. The possibility to simulate non-Abelian anyons using Abelian ones is then considered. Finally, a non-Abelian quantum memory is dissected in order to determine the means by which it provides fault-tolerant storage of information. This understanding is then employed to build equivalent quantum memories with Abelian anyon models. The methodology provides with the means to demonstrate that Abelian models have the capability to simulate non-Abelian anyons, and to realize the same computational power and fault-tolerance as non-

Abelian models.

Apart from the intellectual interest in relating topological models with each other, and of understanding the properties of non-Abelian anyons in terms of the simpler Abelian ones, these results can also be applied in the lab. The simpler structure of Abelian anyons means that their physical realization is more straightforward. The demonstration of non-Abelian properties with Abelian models therefore allows features of non-Abelian anyons to be realized with present and near future technology. Based on this possibility, proposals are made here for proof of principle experiments.

Contents

List of Figures

List of Symbols

$\sigma^x, \sigma^y, \sigma^z$	Pauli operators acting on lattice spins.
X, Y, Z	Pauli operators acting logical qubits or qudits.
$\left\|\, g\right\rangle, \left\|\, \tilde{g}\right\rangle$	Eigenstates of σ^z (or Z) and σ^x (or X) respectively.
F	Fourier transform acting on lattice spins or qubits.
$A^g(v), B^g(p)$	Vertex and plaquette operators on lattice spins, raised to the power $g \in Z_d$.
R_g, L_g	Lattice spin operators, for right and left multiplication by $g \in S_3$, respectively.
$T_g(v)$	Vertex operator on lattice spins for element $g \in S_3$.
$P_a(v)$	Projector onto states in which the vertex v holds an anyon of type a.
W_i^a	Operator acting in spin i to create an a, $\overline{a}$ pair.
$N_{a,b}^c$	The multiplicity for the fusion of anyons a and b to c.
$R^{a,b}$	The braid matrix for anyons a and b.
$F_{a,b,c}^d$	The matrix for the fusion of anyons a, b and c to d.
d_a	The quantum dimension of an anyon a.
D	The total quantum dimension of an anyon model.
$D(G)$	Quantum double model based on the group G.
Z_d	Cyclic group of order d.
S_3	The permutation group of three objects.
ω^g	A complex root of unity, raised to the power h.
t	A generator of S_3, representing the transpose of the three objects.
c	An generator of S_3, representing a cycle of the three objects.

List of Quasiparticles

1	The vacuum particle type in an anyon model.
e^g	Charge anyon of $D(Z_d)$. Equivalent to the fusion of g of the e^1 anyons for $g \in Z_d$.
m^g	Flux anyon of $D(Z_d)$. Equivalent to the fusion of g of the m^1 anyons for $g \in Z_d$.
$\epsilon^{g,h}$	Composite anyon of $D(Z_d)$. Equivalent to the fusion of an e^g and m^h.
e	Charge anyon of $D(Z_2)$.
m	Flux anyon of $D(Z_2)$.
ϵ	Composite fermion of $D(Z_2)$.
Φ	Anyon of $D(S_3)$.
Λ	Anyon of $D(S_3)$.
$\tilde{\Phi}$	Quasiparticle of the enhanced $D(Z_6)$ model of Chapter 4.
$\tilde{\Lambda}$	Quasiparticle of the enhanced $D(Z_6)$ model of Chapter 4.
$\phi, \overline{\phi}$	Quasiparticles of the enhanced $D(Z_6)$ model of Chapter 5.
λ	Quasiparticle of the enhanced $D(Z_6)$ model of Chapter 5.
$\chi, \overline{\chi}$	Quasiparticles of the enhanced $D(Z_6)$ model of Chapter 5.
μ	Quasiparticle of the enhanced $D(Z_6)$ model of Chapter 5.
σ	Anyon of the Ising model.
ψ	Anyon of the Ising model.
$\tilde{\sigma}$	Quasiparticle of an enhanced $D(Z_2)$ model.
$\tilde{\psi}$	Quasiparticle of an enhanced $D(Z_2)$ model.

Chapter 1

Introduction

This thesis is about anyons, Abelian and non-Abelian, and their use in quantum computation. I[1] aim to demonstrate the power of Abelian anyons, showing that these humble quasiparticles have the same potential for fault-tolerant universal quantum computation as their non-Abelian counterparts. Not only this, they do so without demanding as much from the experimentalist.

In order to achieve this aim I take a spin lattice model used to realize non-Abelian anyons, pull it apart to see how it works, and then put it back together again. In doing so I find that the non-Abelian group structure underlying these models is an unnecessary complication. It can be removed without compromising fault-tolerance or computational power, while making the models more tractable theoretically and experimentally.

But before we embark upon this study, there are questions that must be answered. What are anyons? What does it mean when we say they are Abelian or non-Abelian? And what does either have to do with quantum computation? The particles known as anyons are those that are neither bosons or fermions, but which can have any exchange statistics, hence 'any'-ons[2] [5, 6]. The so-called Abelian anyons are straightforward generalizations of their bosonic and fermionic cousins,

[1] Or 'we' as I will refer to myself in the following chapters, having no stomach for the first person singular in academic writing.

[2] It troubles me sometimes, in the depths of the night, that I have spent four years working in a field based upon a bad pun.

since their exchange can yield only a phase factor. For non-Abelian anyons, however, exchanges can yield unitary operations.

It was Kitaev who realized that the properties of non-Abelian anyons make them well suited to the job of quantum computation [7]. The space on which the exchange operations act, known as the fusion space, is inaccessible to local or LOCC operations. This makes it the perfect place to store quantum information away from environmental noise. The implementation of gates by braiding the anyons is also robust against errors, since the fusion space is only sensitive to the topology of their paths. These encouraging properties led to the founding of a new field of research, that of topological quantum computation [8].

But what topology giveth, it also taketh away. Though it supplies us with intrinsically resilient quantum computation, it does not allow anyons to exist in our three-dimensional universe. Hence, rather than just catching a few wild anyons and harnessing them for the next generation of computers, we must endeavour to create them as quasiparticles in two-dimensional systems. The fractional quantum Hall effect was the first means found to do this [9–11], with spin lattice models proposed some years later [7, 12, 13].

The last decade has seen an explosion of work in the field of anyons. Their abstract theory has been explored and extended [14–18], and a large number of models have been catalogued [19]. The systems on which they may be realized have been probed extensively [20–27], with experiments explicitly demonstrating Abelian anyons [28–32] and providing evidence for non-Abelian ones [33]. Their uses for quantum computation have been explored [34–43], and efficient algorithms have been designed [8, 44]. Numerous reviews have also been written [45–47]. It is to this body of work that this thesis belongs, contributing to the understanding of anyons in general, how they may be used, the means by which they may be realized and the experiments that may be done to demonstrate their existence.

Within this thesis, I introduce two new concepts to the field of topological quantum computation. Firstly I introduce the concept of enhanced Abelian models, and

their associated enhanced Abelian quasiparticles. These are the means by which Abelian anyons may be reinterpreted such that they appear to have similar properties to, and can perform some of the tasks of, non-Abelian anyons. They are introduced in full in Chapter 4. Secondly I introduce the concept of non-abelian-like memories for encoding quantum information. These are memories that can be used both with non-Abelian and enhanced Abelian models. Like the quantum memories usually associated with non-Abelian anyons, these are defined using the fusion space. The differences lie in the means by which the stored information may be manipulated, and the steps that must be taken to ensure full fault-tolerance. These memories are introduced in full in Chapter 5.

The thesis is structured as follows:

- Chapter 2 introduces the background required for the thesis. An introduction to the abstract theory of anyons is given, as well as the definition of the quantum double models that can be used to realize them. The theory of topological quantum computation is then presented.

- Chapter 3 deals with my work on the use of Abelian anyon models for the task of quantum computation. Since these models are not universal by braiding alone they, like non-universal non-Abelian models, require the addition of non-topological operations. Various such gate sets are considered and their power analysed, with universality proven in certain cases. The chapter is based on the work presented in [1], done in collaboration with Jiannis K. Pachos.

- In Chapter 4 I present my work in demonstrating that non-Abelian anyons can be simulated using Abelian ones, including realizations of non-trivial fusion and braiding behaviour as well as simulating chirality from a non-chiral model. The general methodology used to do this is presented, and will be used throughout the thesis. This chapter is mostly based upon the work presented in [2], which was done in collaboration with Ville Lahtinen, Zhenghan Wang and Jiannis K. Pachos. It also includes elements discovered in the studies of the next chapter.

- Chapter 5 is a study of a quantum memory based on the non-Abelian charge anyons of the $D(S_3)$ model. Different methods of encoding are found which, though very similar seeming on the surface, have markedly different properties. The reasons for the similarities and differences are then explored. These studies are then applied to an Abelian model, where it is shown that equivalent quantum memories can be realized. Methods to ensure the fault-tolerance of this encoding are then developed, applicable in both Abelian and non-Abelian models. This chapter is based on the work presented in [3] and [4], both done in collaboration with Ville Lahtinen and Jiannis K. Pachos, with the latter also involving Benoit Doucot.

- Chapter 6 then draws together the theoretical arguments of the previous chapters in order to propose experimental implementations. Where possible, each scheme is distilled down to its basics so that proofs of principle may be realistically carried out in the lab. This chapter also includes elements of the work presented in [4].

- Finally, in Chapter 7, I conclude. The results of all previous chapters are shown to achieve our aim of proving that Abelian anyons are as good for quantum computation as their non-universal non-Abelian counterparts. Other results uncovered along the way are also discussed.

So now, let us begin with the quest!

Chapter 2

Anyons and quantum double models

In this chapter the theoretical and experimental background to the thesis is presented. Firstly the abstract theory of anyons is introduced in Section 2.1. Then the anyon models explored in the thesis are presented, along with the spin lattice models used to realize them. Firstly the quantum double models are given, with the Abelian case in Section 2.2 and a particular example of a non-Abelian model in Section 2.3. Kitaev's honeycomb lattice model is then presented in 2.4, with the associated Ising anyon model. Finally, in Section 2.5, it is shown how anyons may be used for quantum computation, and why this is said to be topologically protected.

2.1 The theory of anyons

The definition of an anyon model is a process of several stages [45]. Firstly a set of particle types is defined for the anyons, with one always defined to be the trivial vacuum particle type, 1. This list of possible particle types within the model must be exhaustive, such that even when two or more particles are combined, their composite must also behave according to one of the defined particle types. To systematically describe this process, known as the fusion of the particles, fusion rules are defined. These determine which possible outcomes, known as fusion channels, can occur for

a given composition of particles.

The fusion rules of a model take the form,

$$a \times b = \sum_c N_{a,b}^c \, c. \tag{2.1}$$

This denotes the fusion of particles of type a and b to yield one of type c. The $N_{a,b}^c$ are fusion multiplicities which can be any non-negative integer. For $N_{a,b}^c = 0$ there is no way in which a and b can fuse to a particle of type c. For $N_{a,b}^c > 0$ the fusion is possible in $N_{a,b}^c$ distinguishable ways.

Such multiplicities may also be defined for fusions of more than two anyons. For example, consider the fusion of anyons a, b and c to an anyon of type d. Though the fusion channel of all three anyons is fixed, the intermediate fusion outcomes are not. Hence, if a and b are first fused, the outcome e can take many possible values. Similarly, if b and c are first fused the outcome e' can take multiple values. The multiplicity for the fusion of the three anyons can then be defined,

$$N_{a,b,c}^d = \sum_e N_{a,b}^e N_{e,c}^d = \sum_{e'} N_{b,c}^{e'} N_{a,e'}^d. \tag{2.2}$$

Multiplicities for larger numbers of anyons can be defined similarly.

The space of states describing how given collection of anyons will fuse to a given outcome is known as the fusion space of the anyons. The basis states are labelled by each of the possible intermediate fusion outcomes, with each different order of fusion corresponding to a different basis. The dimension of the fusion spaces is therefore equal to the corresponding multiplicity. The fusion space of anyons is a non-local property, which cannot be accessed by local or LOCC operations on the anyons. Only the braiding or interaction of anyons can have an effect on the fusion space.

The full description of an anyon model requires operations on the fusion space, known as F- and $R-$ matrices, to be defined. The former acts on the fusion space of the three anyons a, b and c and determines the relationship between the two possible fusion bases. A depiction of its definition can be found in Fig. 2.1 (a).

The R-matrix describes the effect of exchanging anyons. It acts on the fusion space of two anyons, a and b, mapping it to to the space for which their positions are exchanged, and hence that of the two anyons b and a. In addition it may also place a complex phase on the wave function of the anyons, depending on their particle types and fusion channel. In the case of non-Abelian anyons the multiplicity of fusion channels means that braiding can implement non-trivial unitary operations on the fusion space. A depiction of the action of this matrix can be found in Fig. 2.1 (b). Note that the F- and R-matrices of a model cannot be chosen arbitrarily, but must satisfy consistency relations known as the pentagon and hexagon relations [48]. Once the F- and R-matrices are chosen from the set of possibilities that are consistent with the fusion rules, the definition of the anyon model is complete.

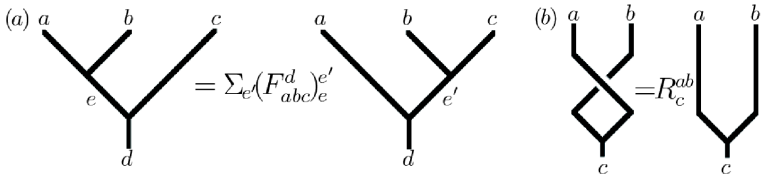

Figure 2.1: The (a) F-matrix and (b) R-matrix of an anyon model. The states of the fusion space are depicted by diagrams showing the corresponding fusions, with time flowing downwards.

An important quantity describing the anyons of a model is their quantum dimension. The quantum dimension of an anyon a is denoted d_a. This can be thought of as the fraction of the fusion space carried by each anyon, and is defined according to the fusion rules as follows,

$$d_a d_b = \sum_{a,b,c} N^c_{a,b} d_c. \tag{2.3}$$

Once calculated for each particle type, the quantum dimensions can used to define the total quantum dimension, D, of the model,

$$D = \sqrt{\sum_a d_a^2}. \tag{2.4}$$

This quantity is related to the entanglement of a physical medium on which an anyon model may be realized. The most natural measure of entanglement for such systems is the topological entropy, γ, for which it has been shown that a model with total quantum dimension D requires a state with entanglement $\gamma = \log D$ [14, 15].

Anyon models are split into two classes: Abelian and non-Abelian. Abelian models are a restricted class in which all fusions have only one possible outcome, and so all fusion spaces are one dimensional. Fusion rules therefore simplify to,

$$a \times b = c. \tag{2.5}$$

The braiding of Abelian models is described by R-matrices acting on one-dimensional spaces, and so yields only global phases on the wave function. Non-Abelian models are the more general class. Multiple fusion outcomes are allowed and fusion spaces are can be non-trivial. Since the braiding of non-Abelian anyons acts on spaces greater than one-dimension it can therefore implement unitary operations.

Since the theory of anyons describes the fusion space as a perfectly general Hilbert space, the implementation of operations beyond those of braiding and fusion can be considered. The effect these have on the fusion space, and hence the fusion behaviour of the anyons, can therefore be fully predicted from the anyonic theory.

Simulations of anyons

No anyons are known to exist in the universe, and none are expected to exist. However, their properties would make them ideal for quantum computation, as will be described later in Section 2.5. It is therefore desirable for us to simulate anyons in order to benefit from their unique behaviour. Certain systems have proven to be well suited to this task, with the ability to produce quasiparticles that reproduce anyonic behaviour.

These simulations can never be perfect, since certain operations on the underlying physical systems may affect the behaviour of the quasiparticles in ways not consistent with anyonic theory. Any such simulation is therefore only as good as the

restrictions that must be made such that it is valid. Harnessing the full power of anyons therefore requires a full knowledge of the properties and limitations of the simulations.

The quantum double models considered in this thesis are a means by which simulations of certain anyon models may be realized on two-dimensional spin lattices [7]. They allow the fusion space to be realized as a non-local property of the quasiparticles, and the application of non-topological operations will yield the effects predicted by the anyonic theory. However, it is important to know their limitations. As we will see in Chapter 5, the non-locality of the fusion space holds true only as long as the operations are implemented in the correct way. Other operations, which naively seem to yield the same effects, can lead to the fusion space becoming accessible to LOCC measurements. Also, though these models realize all full monodromies in braiding, the effects of single exchanges are not always realized exactly as they should be according to anyon theory.

2.2 Abelian quantum double models

The quantum double models are a particular spin lattice realization of certain anyon models [7]. Each is based on a group, with the quantum double of a finite group G denoted $D(G)$. Anyons are associated with states of the spins around each plaquette and vertex, with plaquette anyons known as fluxes and vertex anyons called charges. The fusion and braiding behaviour of the anyons depends on the property of the group employed. For example, an Abelian group leads to Abelian anyons, and a non-Abelian group to non-Abelian anyons.

Quantum double models can be defined on spin lattices, with groups of order d requiring a lattice of d-level spins. The $D(Z_2)$ model, more commonly known as the toric code [34, 35], is defined on a $d = 2$ lattice and is a well-known example of a stabilizer code [49]. For other d the models correspond to higher dimensional generalizations of the stabilizer code concept.

In this section, Abelian quantum double models are presented in detail. First

the models based upon the cyclic groups Z_d are considered [50], followed by the generalization to all Abelian groups.

Quantum double models of cyclic groups

Consider the cyclic group of d elements, Z_d. We label the elements of this group $\{0, 1, \ldots, d-1\}$. This allows us to represent the binary operation as addition modulo d, hence for two elements g and h,

$$g \times h = g + h \pmod{d}.$$

A quantum double model based on such a group can be realized on a square lattice with a d-level spin on each edge. The elements of Z_d are used to label the basis states of the spins. Generalized Pauli operators are defined,

$$\sigma^x = \sum_{h \in Z_d} |\, h + 1 \,(\mathrm{mod}\, d)\rangle \langle h\,|\,, \quad \sigma^z = \sum_{h \in Z_d} \omega^h \,|\, h\rangle \langle h\,|\,, \tag{2.6}$$

where $\omega = e^{i2\pi/d}$. These satisfy the commutation relation $\sigma^z\sigma^x = \omega\sigma^x\sigma^z$. The eigenstates of σ^x are those of the Fourier transform basis,

$$|\,\tilde{g}\rangle = \frac{1}{\sqrt{d}} \sum_{h \in Z_d} \omega^{gh} \,|\, h\rangle\,, \tag{2.7}$$

with corresponding eigenvalues ω^{-g}. To rotate between these two bases, the following unitary is used to perform the Fourier transform,

$$F = \sum_{h \in Z_d} \left|\, \tilde{h} \right\rangle \langle h\,| = \frac{1}{\sqrt{d}} \sum_{g,h \in Z_d} \omega^{gh} \,|\, h\rangle \langle g\,|\,. \tag{2.8}$$

This has the properties $F^2\,|\,g\rangle = |\,-g\rangle$, $F^3 = F^\dagger$ and $F^4 = I$. Here, due to the use of cyclic groups, $-g$ is taken to mean $d - g$.

The stabilizers of the quantum double models are defined as follows on the four

spins around each vertex, v, and plaquette, p,

$$A(v) = \sigma_1^{x\dagger}\sigma_2^{x\dagger}\sigma_3^x\sigma_4^x, \;\; B(p) = \sigma_1^{z\dagger}\sigma_2^z\sigma_3^z\sigma_4^{z\dagger}, \tag{2.9}$$

where the numbering proceeds clockwise from the top-most spin (Fig. 2.2). These have eigenvalues $\omega^g = e^{i2\pi g/d}$ for each $g \in Z_d$. For a system in an arbitrary state $|\,\psi\rangle$, no anyon is associated with a vertex or plaquette if $A(v)\,|\,\psi\rangle = B(p)\,|\,\psi\rangle = |\,\psi\rangle$. An anyon e^g is associated with a vertex, v, if $A(v)\,|\,\psi\rangle = \omega^g\,|\,\psi\rangle$. An anyon m^h is associated with a plaquette, p, if $B(p)\,|\,\psi\rangle = \omega^h\,|\,\psi\rangle$. The presence of both in an adjacent plaquette and vertex is associated with the composite particle $\epsilon^{g,h}$. The anyonic vacuum corresponds to the stabilizer space of the code.

Projectors onto the states of anyons can be constructed from the plaquette and vertex operators as follows,

$$P_{e^g}(v) = \sum_{g\in Z_d} \omega^g A(v), \;\; P_{e^g}(p) = \sum_{g\in Z_d} \omega^g B(p). \tag{2.10}$$

Using these, a Hamiltonian may be defined whose ground state corresponds to the anyonic vacuum,

$$H = -\sum_v P_{e^0}(v) - \sum_p P_{m^0}(p). \tag{2.11}$$

Since this Hamiltonian projects onto the vacuum for all plaquettes and vertices, it acts in the same way to all states that do not correspond to the vacuum. Hence it assigns equal energy to all e^g and m^g anyons, without distinguishing their type. Since the anyons are localised excitations, they may be thought of as quasiparticles.

The resulting anyon model is then as follows.

- *Particle types:*

$$e^g, \;\; m^g, \;\; \epsilon^{g,h} \;\; \forall g, h \in Z_d. \tag{2.12}$$

  Where $e^0 = m^0 = \epsilon^{0,0} = 1$.

- *Fusion rules:*

$$e^g \times e^h = e^{g+h(\mathrm{mod}\, d)},\ m^g \times m^h = m^{g+h(\mathrm{mod}\, d)},\ e^g \times m^h = \epsilon^{g,h}. \tag{2.13}$$

- *R-matrices:*

$$(R^{e^g m^h}_{\epsilon^{g,h}})^2 = \omega^{gh},\ \omega = e^{i2\pi/d}, \tag{2.14}$$

  with all others trivial.

- *F-matrices:* All trivial.

The creation and movement of the anyons may be achieved by σ^z and σ^x operations on the spins of the lattice, as depicted in Fig. 2.2. The creation of any anyon e^g or m^g will result also in the creation of its respective antiparticle, e^{-g} or m^{-g}. The operation $(\sigma^z)^g$ on spins 1 or 2 of a vertex, or $(\sigma^z)^{-g}$ on 3 or 4, creates an e^g charge at that vertex and an e^{-g} on the other vertex shared by the spin. Similarly, a $(\sigma^x)^g$ on spins 2 or 3 of a plaquette, or a $(\sigma^x)^{-g}$ on 1 or 4, creates an m^g flux on that plaquette and an m^{-g} on the other plaquette shared by the spin. Particles can be moved and braided using corresponding strings and loops of the σ^z and σ^x operations. The commutation relations of these give a phase ω^{gh} when an e^g anyon is moved clockwise around an m^h. The phase ω^{-gh} is obtained for an anticlockwise braiding.

Abelian models in general

All Abelian groups are either cyclic, or direct products of cyclic groups. Since we have already dealt with quantum double models based upon the former, we need only consider the latter.

Consider a group $Z_{d_1} \times Z_{d_2}$, the direct product of two arbitrary cyclic groups. The $D(Z_{d_1} \times Z_{d_2})$ model may be realized on a square lattice with two spins at each edge, one a d_1-level spin and the other a d_2-level spin. On the former spins

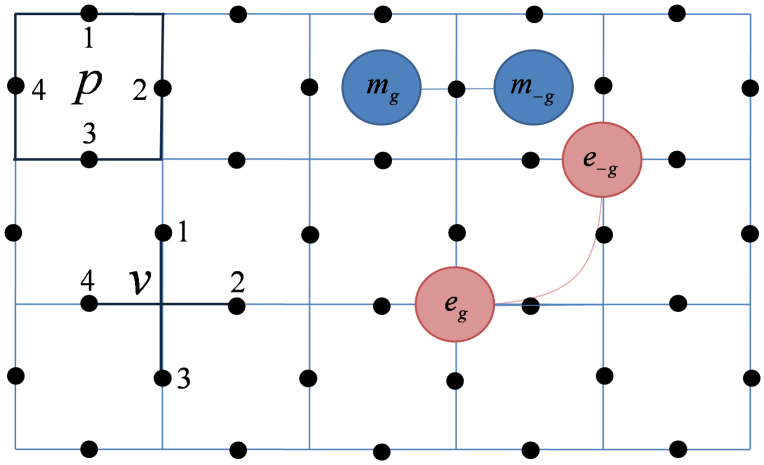

Figure 2.2: The quantum double models are realized on a square lattice with a d-level spin on each edge. A numbering of the spins around each plaquette, p, and vertex, v, is given. Anyons e^g reside on vertices. These may be created in pairs by single spin operations, and moved away from each other by further single spin operations. Anyons m^g reside on plaquettes, and may be created and moved similarly.

the quantum double model $D(Z_{d_1})$ may be defined as above, and on the latter the model $D(Z_{d_2})$ may be defined. The anyons of $D(Z_{d_1} \times Z_{d_2})$ therefore do not admit any behaviour beyond those of $D(Z_{d_1})$ and $D(Z_{d_2})$ alone, it merely allows them to be realized on the same lattice. Corresponding arguments apply to direct products of three or more cyclic groups.

The only difference between the model $D(Z_{d_1} \times Z_{d_2})$ and independent realizations of $D(Z_{d_1})$ and $D(Z_{d_2})$ concerns the Hamiltonian, as defined in Eq. 2.11. The Hamiltonian of $D(Z_{d_1} \times Z_{d_2})$ assigns equal energy to an anyon e^g from $D(Z_{d_1})$, e^h from $D(Z_{d_2})$, and the combination $e^g e^h$ of the two. This would not be the case if the $D(Z_{d_1})$ and $D(Z_{d_2})$ Hamiltonians were applied independently, as $e^g e^h$ in this case would be assigned energy by each independent Hamiltonian, and thus have twice the energy.

2.3 The non-Abelian $D(S_3)$ quantum double model

The structure of non-Abelian quantum double models is far more complex than their Abelian counterparts. For this reason only the charge anyons of the $D(S_3)$ model

are presented here, since only these will be required in this thesis. As such the definition of the model seems quite arbitrary. However, if the reader desires a more holistic understanding, the theory underlying non-Abelian quantum double models is outlined in [7] and a full treatment of $D(S_3)$ can be found in [24].

The spin lattice model

The $D(S_3)$ anyon model is defined on an oriented two-dimensional square lattice. On each edge there resides a six-level spin whose states are labelled by the elements of S_3, the permutation group of three objects. We express every element in terms of generators t and c, which can be understood as the transpose and cycle of the objects. These satisfy $t^2 = c^3 = e$ and $tc = c^2t$, where e denotes the trivial element. Using this notation the six elements are given by $S_3 = \{e, c, c^2, t, tc, tc^2\}$.

The properties of the group can be used to define operations on the spins. The unitary operations $R_g(i)$ and $L_g(i)$ can be used to implement right and left multiplication, respectively, of the state of a spin i by the group element g,

$$R_g \,|\, h\rangle = |\, hg\rangle\,, \quad L_g \,|\, h\rangle = |\, gh\rangle \quad g, h \in S_3 \tag{2.15}$$

These may then be used to define the following operators which act on the four spins around a vertex,

$$T_g(v) = R_g(1)R_g(2)L_{g^{-1}}(3)L_{g^{-1}}(4), \tag{2.16}$$

The choice of which spins are acted upon by R_g and which by $L_{g^{-1}}$ ensures that such operators defined on different vertices will always commute, even when defined for different and non-commuting group elements. A depiction of the operator can be found in Fig. 2.3.

For all purposes in this thesis we consider only the so-called charge anyons associated with the vertices of the lattice, and assume that the plaquettes are fixed in the vacuum state. There are two non-trivial charges, which we call Λ and Φ, and the trivial vacuum charge, 1. For a general state of the system, $|\, \psi\rangle$, the presence

of a charge of type a at vertex v is defined by $P_a \,|\, \psi\rangle = |\, \psi\rangle$, where the orthogonal projectors are given by,

$$\begin{aligned} P_1(v) &= \frac{1}{6}[T_e(v) + T_c(v) + T_{c^2}(v) + T_t(v) + T_{tc}(v) + T_{tc^2}(v))], \\ P_\Lambda(v) &= \frac{1}{6}[T_e(v) + T_c(v) + T_{c^2}(v) - T_t(v) - T_{tc}(v) - T_{tc^2}(v)], \\ P_\Phi(v) &= \frac{1}{3}[2T_e(v) - T_c(v) - T_{c^2}(v)]. \end{aligned}$$

Projectors are also defined for the states of flux anyons on plaquettes, but we need not give them here.

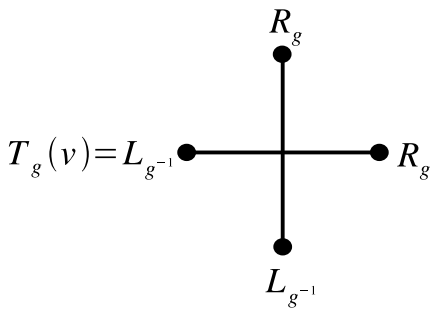

Figure 2.3: A pictorial representation of the vertex operators $T_g(v)$.

The stabilizer space consists of states with no anyons, i.e. those for which $P_1(v) \,|\, \psi\rangle = |\, \psi\rangle$ for all v, and a similar condition for the fluxes on plaquettes. The syndrome measurement is defined as a measurement of anyon occupancies, and so corresponds to the above projectors. A Hamiltonian may be defined to maintain the stabilizer space. This assigns energy to the states of the anyons, and thus suppresses their spontaneous creation. This may be expressed,

$$H = -\sum_v P_1(v) - \sum_p P_1(p). \tag{2.17}$$

States with no anyons form the ground state of this, and hence may be denoted $|\, \mathrm{gs}\rangle$.

Charge anyons are created from the stabilizer space by acting with the following

operators on single spins,

$$W_i^{\Lambda} = |e\rangle\langle e| + |c\rangle\langle c| + |c^2\rangle\langle c^2| - |t\rangle\langle t| - |tc\rangle\langle tc| - |tc^2\rangle\langle tc^2|, \quad (2.18)$$

$$W_i^{\Phi} = 2|e\rangle\langle e| - |c\rangle\langle c| - |c^2\rangle\langle c^2|. \quad (2.19)$$

These create charges on the two vertices connected sharing the spin i. A protocol to create and move charges apart is given in [24].

The anyon model

The set of charge anyons is closed under fusion, and so they form their own consistent submodel of non-Abelian anyons [43]. The properties of this model are as follows.

- *Particle types:*

$$1,\ \Phi,\ \Lambda. \quad (2.20)$$

- *Fusion rules:*

$$\Phi \times \Phi = 1 + \Lambda + \Phi,\ \Lambda \times \Lambda = 1,\ \Phi \times \Lambda = \Phi. \quad (2.21)$$

- *R-matrices:*

$$R^{\Phi\Phi} = \begin{pmatrix} 1 & 0 & 0 \\ 0 & -1 & 0 \\ 0 & 0 & 1 \end{pmatrix} \quad (2.22)$$

  in the basis 1, Λ, Φ.

- *F-matrices:*

$$F^{\Phi}_{\Phi\Phi\Phi} = \frac{1}{2}\begin{pmatrix} 1 & 1 & -\sqrt{2} \\ 1 & 1 & \sqrt{2} \\ -\sqrt{2} & \sqrt{2} & 0 \end{pmatrix}, \quad (2.23)$$

  in the basis 1, Λ, Φ.

The fusion rules of the Φ anyons demonstrates their non-Abelian nature. However, these anyons have the simplest possible non-Abelian behaviour. Their braiding has no effect on the fusion space other than that required to describe the effect of permuting the anyons.

2.4 The honeycomb lattice model

Kitaev's honeycomb lattice is a spin lattice model that can be used to realize certain anyon models [51]. Unlike the quantum double models, its Hamiltonian is frustrated, making it much more difficult to solve explicitly in terms of the underlying spin lattice. This is especially true for the non-Abelian phase of the model, for which the states of the anyon cannot yet be expressed in terms of the states of the underlying spins.

The model is defined on a hexagonal lattice, as shown in Fig. 2.4. A spin-1/2 particle is located at each vertex of the lattice, with edges labelled x, y and x according to orientation. The Hamiltonian is then defined,

$$\begin{aligned} H &= J_x H_x + J_y H_y + J_x H_z + iK\left[H_x, H_y\right], \\ H_\alpha &= \sum_{\alpha-links} \sigma_i^\alpha \sigma_j^\alpha. \end{aligned} \tag{2.24}$$

Here the J_x, J_y, J_z and K are positive coupling strengths and $\alpha \in \{x, y, z\}$.

For each plaquette of the lattice, P, there is defined a plaquette operator,

$$W_P = \sigma_1^x \sigma_2^y \sigma_3^z \sigma_4^x \sigma_5^y \sigma_6^z. \tag{2.25}$$

For an arbitrary state $|\,\psi\rangle$, there is said to be a vortex on the plaquette P if $W_P\,|\,\psi\rangle = -\,|\,\psi\rangle$. The W_P operator commutes with the Hamiltonian, and so the number and positions of the vortices are conserved under its action.

When $K = 0$ and $J_z \gg J_x, J_y$, perturbation theory shows that the Hamiltonian is effectively equal to that of the $D(Z_2)$ model. The vortices then become the

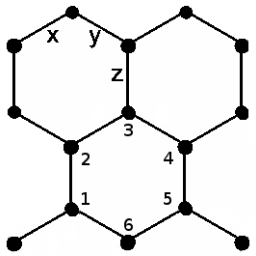

Figure 2.4: The hexagonal lattice on which Kitaev's model is defined. The numbering of spins around a plaquette is shown.

anyons, with e's and m's residing on alternate rows of plaquettes. For $K > 0$ and $J_z = J_x = J_y$, the vortices correspond to the non-Abelian anyons of the Ising model, presented below. The Hamiltonian in this case is too complex to diagonalize directly, and so the technique of Majorana fermionization is used. However, this makes it difficult to translate the results back into the spin lattice picture. The non-Abelian phase of the model is therefore not well understood in terms of the underlying spins.

The Ising anyon model

The Ising anyon model is one of the simplest non-Abelian models. The properties of the model relevant for the studies of this thesis are as follows.

- *Particle types:*

$$1,\ \sigma,\ \psi. \tag{2.26}$$

- *Fusion rules:*

$$\sigma \times \sigma = 1 + \psi,\ \psi \times \psi = 1,\ \sigma \times \psi = \sigma. \tag{2.27}$$

- *R-matrices:*

$$R_1^{\psi\psi} = -1,\ (R_\sigma^{\psi\sigma})^2 = -1,\ (R^{\sigma\sigma})^2 = e^{-i\pi/4} \begin{pmatrix} 1 & 0 \\ 0 & -1 \end{pmatrix}, \tag{2.28}$$

  in the basis 1, ψ.

- *F-matrices:*

$$F^{\sigma}_{\sigma\sigma\sigma} = \frac{1}{\sqrt{2}} \begin{pmatrix} 1 & 1 \\ 1 & -1 \end{pmatrix}, \tag{2.29}$$

  in the basis 1, ψ.

As mentioned above, the non-Abelian σ anyons correspond to the vortices of the honeycomb lattice model, as detected by the plaquette operator W_P. The exact nature of the fermions ψ in terms of the underlying spins of this model is as yet unknown.

2.5 Topological quantum computation

The fusion space of non-Abelian anyons provides the perfect place to store quantum information [7, 8, 46, 47]. Errors can only occur when the anyons used to store the information are braided around or interacted with each other. These processes are efficiently suppressed by keeping the anyons far apart. The braiding of anyons also provides the perfect means to process quantum information, since the operations they perform on the fusion space are implemented exactly and without error. Minor perturbations in the path of the anyons as they moved have no effect on the final operation. The fusion space is sensitive only to the topology of paths, which should not be affected by local perturbations as long as the anyons are kept well separated. However, most Abelian anyon models cannot implement universal quantum computation by braiding alone. Other, so-called non-topological operations must be used in addition, which do not have the same resilience to errors as braiding [39–41]. These are achieved by bringing anyons close together and interacting them by some means. Since such operations are beyond those natural to the anyon models, the means by which they may be implemented and the practicality of their use depends on the physical system used to realize the anyons.

Abelian anyon models can also be used for topological quantum computation. Since quantum double models are stabilizer codes, quantum information can be stored in the stabilizer space of Abelian models. The most famous example of

this is the toric code, for which the $D(Z_2)$ model is realized on a square lattice wrapped around a torus [34, 35]. Logical operations can be performed by moving anyons through topologically non-trivial paths. As long as the size of the code is large, this protects against errors in a similar way to encoding in the non-Abelian fusion space. The gate set achieved by moving the anyons is not universal, so non-topological operations are required. However, since the information is not stored on anyons which may be moved close and interacted, as in the non-Abelian case, the implementation of such operations becomes highly impractical. An exception to this is found in measurement based schemes inspired by quantum double models, but based on cluster states. In these, quantum information can be stored in 'holes' in the code [42]. The braiding of the holes then allows quantum computation in a way similar to non-universal non-Abelian models. However, though such holes can also be defined for the quantum double models realized in the usual way on two dimensional lattices, the means to move them without error is not known. This is especially true when the holes are made large enough to support fault-tolerance, since the problem of impracticality again arises.

The contribution of this thesis to the field is to expand on the means by which Abelian quantum double models may be used for topological quantum computation, and show that their potential is the same as that of non-Abelian models that are not universal by braiding. Chapter 3 deals with the non-topological operations required for universality. Chapter 5 shows that the holes used to encode information may be carried by quasiparticles, and hence we can expect that they can be moved in a similar way as non-Abelian anyons.

Chapter 3

A toolkit for quantum computation with Abelian anyons

The experimental accessibility and control of Abelian anyons is expected to be easier than their non-Abelian counterparts, an expectation supported by current experimental progress [28–33]. Hence, rather than simply rely on non-Abelian anyons in order to implement quantum computation, it is important to understand how well this may be achieved with Abelian models.

Some work has already been done in this direction. Dennis et. al. [35], Lloyd [36] and Pachos [38] have all made proposals for quantum computation with Abelian anyon models. Raussendorf et al. [42], also proposed a measurement based scheme inspired by Abelian anyons. In all these works, only the $D(Z_2)$ model is considered in detail. It is therefore interesting to see how quantum computation may be performed on a more general class of Abelian models.

In this chapter the computational power of Abelian quantum double models is investigated, as are the means that may be used to provide universality. The structure of the chapter is as follows. Firstly, the gates that can be realized by the topological operations of anyon creation, transport and annihilation are determined

in section 3.1. These do not form a gate set useful for quantum computation, but they form the foundation of the operations used in the following sections. Since the quantum double models are realized on a spin lattice, the effect of measuring single spins may be considered. In section 3.2 it is shown that measurements in each Pauli basis are sufficient to realize all Clifford group operations for $D(Z_2)$. This is then extended in section 3.3, where arbitrary single spin measurements are considered on all Abelian quantum double models, with universality proved in certain cases. Finally, in section 3.4 we consider how computation may be achieved without braiding, determining the gates that may be used to achieve universality in this case with minimal resources.

As shown in Chapter 2, all the anyonic behaviour of Abelian quantum double models are contained within those models based upon cyclic groups. Models based based on products of these groups only differ in the spectrum of their Hamiltonian, not the braiding and fusion of the anyons that is important for quantum computation. Hence only cyclic group quantum double models will be considered in the rest of this chapter without loss of generality.

This chapter considers only the computational power of Abelian models, and contains no arguments of fault-tolerance or topological protection. The means by which the computation proposed may be performed in a fault-tolerant manner is explored in Chapter 5, but still remains an open topic for research.

3.1 Gates implemented with topological operations alone

The operations of anyon creation, transport and fusion would be expected to come naturally for any realization of an anyonic model. Hence we begin by considering how quantum information is most naturally encoded in an Abelian model, and what gates can be achieved through these basic operations. This forms the foundation of the schemes in the following sections.

Encoding of logical qudits

In order to determine what gates may be achieved using Abelian models, the encoding of information must first be defined. Logical qudits are stored using 'holes': plaquettes or vertices on which the relevant terms in the Hamiltonian are removed, and hence the stabilizers are not enforced [42]. Any quantum double model based on a cyclic group, $D(Z_d)$, may be used to store a d level qudit in two vertex holes, v_1 and v_2, as follows,

$$|\, j\rangle_v = \left|\, e^j\right\rangle_{v_1} \left|\, e^{-j}\right\rangle_{v_2}. \tag{3.1}$$

Here $\left|\, e^j\right\rangle_{v_1}$ represents the state for which the the vertex hole v_1 contains an anyon e^j, etc. The basis state $|\, j\rangle$ therefore corresponds to a state in which an anyon e^j resides in the hole v_1 and its antiparticle in v_2. Since this qudit is stored in vertex holes, it is referred to as a v-type qudit. Plaquette holes may be used to store p-type qudits similarly,

$$|\, j\rangle_p = \left|\, m^j\right\rangle_{p_1} \left|\, m^{-j}\right\rangle_{p_2}. \tag{3.2}$$

Note that, since the two holes will hold anyons of different types, it is important to remember which hole is which. Otherwise a qudit in state $|\, g\rangle$ might be mistaken for one in state $|\, -g\rangle$.

Implementation of Pauli operators

Generalized Pauli operators for the logical qudits are defined in the same way as for the lattice spins in Eq 2.6,

$$X = \sum_j |\, j+1\rangle \langle j\,|\,, \quad Z = \sum_j \omega^j\, |\, j\rangle \langle j\,|\,. \tag{3.3}$$

We denote X and Z operations on v- and p-type qudits X_v and Z_v, and X_p and Z_p, respectively.

With the qudit encoding defined above, the implementation of these Pauli operators comes simply from the manipulation of anyons. To perform the logical Z_v

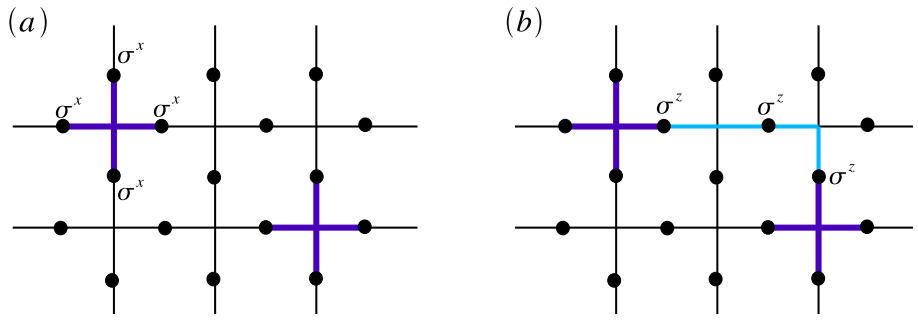

Figure 3.1: A p-type qubit is shown, with the vertex holes coloured dark blue. (a) The logical Z is a product of σ^x operations on the spins around either vertex. (b) The logical X is a product of σ^z operations on spins forming a path between the holes, such as the one coloured light blue.

(Z_p) operation, an m^1 (e^1) must be created and braided clockwise around v_1 (p_1). $Z^\dagger$ can be implemented by instead braiding an m^{-1} (e^{-1}). These logical operations can be expressed in terms of the stabilizers of the model (Eq. 2.9),

$$Z_v = A(v_1) = A^\dagger(v_2),\ Z_p = B(p_1) = B^\dagger(p_2). \tag{3.4}$$

To perform an X_v, an e^1, e^{-1} pair must be created. The e^1 is then placed in the hole v_1 and the e^{-1} in v_2. Similarly an X_p is performed using an m^1, m^{-1} pair. The $X^\dagger$ operation may be implemented in both cases by reversing the destinations of the anyons, placing e^{-1} in v_1, etc. The logical X and Z operations are shown in Fig. 3.1.

Implementation of controlled-Z

If it is assumed that the holes can be moved the gates implemented by braiding can be considered. Braiding the contents of a hole v_1 around a hole v_2 braids the anyons they contain. The phase factor that results will therefore depend on the states of the two qudits,

$$|\, g\rangle_v \,|\, h\rangle_p \to \omega^{gh} \,|\, g\rangle_v \,|\, h\rangle_p \,. \tag{3.5}$$

The resulting gate is the controlled-Z, the qudit generalization of the controlled phase. This implements Z^g on the target qudit when the control is in state $|\,g\rangle$. The gate is completely symmetric, in that either qudit could be viewed as the control or target.

3.2 Clifford gates using Pauli spin measurements

Since the gates above do not form a useful gate set, additional operations must be considered. Here we determine the effect of measuring lattice spins in the basis of Pauli operators σ^x, σ^y and σ^z. This is done in detail for the case of logical qubits stored in the $D(Z_2)$ model, where it is shown that the full Clifford group of gates may be implemented. This makes the model as some non-universal non-Abelian models, such as that of the much celebrated Ising anyons [51]. The case of general $D(Z_d)$ models is then commented upon.

Measuring logical Pauli operators

For the case of the $D(Z_2)$ model, a v-type qubit is stored on two vertex holes, v_1 and v_2, as follows,

$$|\,0\rangle_v = |\,1\rangle_{v_1}\,|\,1\rangle_{v_2}\,,\;\; |\,1\rangle_v = |\,e\rangle_{v_1}\,|\,e\rangle_{v_2}\,.$$

Logical states for p-type qubits take a similar form.

Using measurements of the spin Pauli operators σ^x, σ^y and σ^z it is possible to measure the logical Pauli operators X, Y and Z of the encoded qubits. We first consider this for the logical Z operations, which for the $D(Z_2)$ model take the form,

$$Z_v = A(v_1) = A(v_2),\;\; Z_p = B(p_1) = B(p_2). \tag{3.6}$$

These are four-body operations measuring the parity of spins in the σ^x and σ^z bases, respectively. The logical Z acting on one hole for a v-type qubit is shown in Fig. 3.1(a). Ideally, measurement of the logical Z requires an entangling measurement

of the four spins involved. However, single spin measurements may also be used. To do this one simply measures in the σ^z or σ^x basis of each lattice spin surrounding v_1 or p_1, respectively, and then computes the parity to determine the result. These measurements can also be used to prepare qudits in the $Z_{v/p}$ basis states, $\{|0\rangle_{v/p}, |1\rangle_{v/p}\}$.

Note that measurements performed in such a way will create unwanted anyons. For example, the measurement of the four σ^x's on each spin around a vertex does not commute with the $B(p)$ operators on the surrounding plaquettes. This creates a superposition of m anyons on these plaquettes. Any attempt to correct this by fusing the anyons will only succeed with a probability of $1/2$. Otherwise a logical Z error will be implemented on the qubit. However, since the post-measurement state is an eigenstate of Z, such errors have no effect. Similarly, any attempt to move the hole away from the superfluous anyons will also result in a logical Z error with probability $1/2$, but with no ill effects to the prepared state. These anyons may, however, cause non-trivial errors if allowed to propagate away from their initial position, either by thermal errors or perturbations in the Hamiltonian, and braid around other holes. Any proposal for fault-tolerant computation using these models must therefore include some means to annihilate these.

For measurement of X, consider the case in which the holes are neighbouring. They will then share a lattice spin, i, and the logical X operators take the form,

$$X_v = \sigma_i^z, \; X_p = \sigma_i^x, \tag{3.7}$$

Measurement of the X_v basis is then simply measurement in the σ^z basis of the spin i. Similarly measurement of X_p is measurement of σ_i^x. These measurements may be used to prepare qudits in the $X_{v,p}$ basis states, denoted $\{|\tilde{0}\rangle_{v,p}, |\tilde{1}\rangle_{v,p}\}$.

If the vertices are not neighbouring, the X_v are realized by the product of σ_i^z's on spins that form a path between the two vertices, and the X_p by a product of σ_i^x's between the two plaquettes. This is shown for a p-type qubit in Fig. 3.1(b). Measurement of each logical X can be locally achieved by measuring each spin along

the path in the relevant basis, and computing the parity of results. As with measurement in the Z basis above using a similar technique, this will lead to the creation of unwanted anyons which will cause a logical X error on the post measurement state with probability 1/2. Again, this does not affect X basis preparation.

The logical Y operation may be achieved through a product of X and Z. It is therefore a product of spin Pauli operators that stretch between the holes as well as circling around one. Measurement in the Y basis may again be done locally by measuring each of the single spin Pauli operators, which will again lead to the creation of unwanted anyons. These will independently cause Z and X errors on the post measurement state with probabilities of 1/2. Since these are not eigenstates of the errors, the reliable preparation of Y basis states is not possible.

Implementation of controlled-X

In order to prove that all gates of the Clifford group can be implemented, it must be shown that all such gates can act on both v- and p-types qubits alone. The controlled-Z implemented by braiding does not satisfy this, since it entangles v- type qubits to p-type. However, the controlled-Z can be used to implement a controlled-X on qubits of the same type.

The first step to building the controlled-X is to use the controlled-Z to perform the following operation. Consider a v-type qubit in arbitrary state $|\psi\rangle_v = \sum_j c_j |j\rangle_v$ and a p-type qubit prepared in state $|\tilde{0}\rangle_p = (|0\rangle_p + |1\rangle_p)/\sqrt{2}$. Entangling these together with the controlled-Z yields,

$$\begin{aligned} \Lambda(Z)\,|\psi\rangle_v\,|\tilde{0}\rangle_p &= \frac{1}{\sqrt{2}}(c_0\,|0\rangle_v\,|\tilde{0}\rangle_p + c_1\,|1\rangle_v\,|\tilde{1}\rangle_p) \\ &= \frac{1}{\sqrt{2}}\sum_l |\tilde{l}\rangle_v\,(X_p^l F\,|\psi\rangle_p). \end{aligned} \tag{3.8}$$

Measuring the v qudit in the X_v basis teleports the initial state $|\psi\rangle$ state to the p-type qudit, while implementing the Fourier transform, or Hadamard, F. We denote this process $F_{v\to p}$. This operation is performed up to a Pauli correction, according

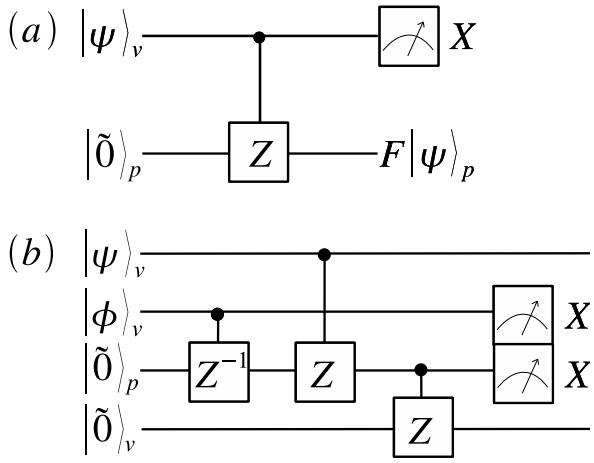

Figure 3.2: Circuits for the implementation of: (a) the Fourier transform with teleportation, $F_{v\to p}$; and (b) the controlled-X. These circuits are shown for the general case of qudits.

to the measurement outcome. A corresponding process $F_{p\to v}$ can be used if the initial state is on a p-type qubit. The circuit for this process is shown in Fig. 3.2 (a).

Using the teleporting Fourier transforms, the controlled-X can be performed between two v-type qubits by first performing $F_{v\to p}$ on the target, then performing the controlled-Z, then finally performing $F_{p\to v}$. The circuit for this process is shown in Fig. 3.2 (b).

Implementation of $Z^{1/2}$, $X^{1/2}$ and F

Since the teleporting Fourier transforms above do not map v-type qubits to v-type, or p-type to p-type, they cannot be used as a Fourier transform in Clifford circuits in a straightforward manner. However, it is possible to implement the gates $Z^{1/2}$ and $X^{1/2}$, which in turn can be used for a standard Fourier transform.

For the implementation of $Z^{1/2}$, consider the implementation of the operation $F_{v\to p}$, as shown in Fig. 3.2 (a). Modifying this such that the measurement of the

first qubit is in the Y basis, rather than the X results, in the state $FZ^{l+1/2}\,|\,\psi\rangle_p$ on the second qubit, where $l \in \{0,1\}$ denotes the measurement result. This implements either $Z^{1/2}$ or its inverse depending on l and then teleports the state from a v to a p-type qubit while implementing the Fourier transform. If $F_{v\to p}$ is then performed as normal the state is teleported back to a v-type qubit, and the Fourier transform is cancelled. The result of the whole process is then the operation,

$$|\,\psi\rangle_v \to Z^{l+1/2}\,|\,\psi\rangle_v\,, \tag{3.9}$$

which simply implements either $Z_v^{1/2}$ or its inverse according to the result of the Y measurement. To apply either deterministically a Z_v can be applied to map $Z_v^{1/2}$ to its inverse and vice-versa. The $X_v^{1/2}$ may be similarly implemented using $F_{p\to v}Z_p^{1/2}F_{v\to p}$. Corresponding processes can be used to perform these operations on p-type qubits.

Implementation of Clifford group

It is well known that the Clifford group is generated by F, $Z^{1/2}$ and the controlled-X [49]. The implementation of the latter two on the $D(Z_2)$ model are explicitly given above. It is therefore sufficient to demonstrate that a Fourier transform can be performed that acts only on a single qubit type, without teleporting between them. This can be constructed according to the relation,

$$F = Z^{1/2}X^{1/2}Z^{1/2}. \tag{3.10}$$

All the required generators can then be performed on either v- or p-type qubits alone, leading to the full Clifford group realized on each.

Generalization of the methods

This result is not limited to the case of $d = 2$, but is true whenever $d = 2d_o$, where d_o is odd. In this case we may encode logical qubits in a subset of e anyons as follows,

$$|\,0\rangle_v = |\,1\rangle_{v_1} |\,1\rangle_{v_2}\,, \quad |\,1\rangle_v = \left|\, e^{d_o} \right\rangle_{v_1} \left|\, e^{d_o} \right\rangle_{v_2}. \tag{3.11}$$

The encoding for p-type qubits is similarly defined. All methods above may be easily applied to this encoding, with the substitution,

$$\sigma^\alpha \to (\sigma^\alpha)^3, \quad \alpha \in \{x, y, z\}. \tag{3.12}$$

Note that the reason that d_o must be odd is for the controlled-Z to be implemented upon braiding. Otherwise this braiding is trivial.

For all other $D(Z_d)$ models the measurements of $X^a Z^b$ operations, generalizations of Y, do not lead to $Z^{1/2}$ or $X^{1/2}$. The gate set realized does not seem to correspond to one that is well studied, and so the computational power remains an open question. It is not known whether they implement the Clifford group or not.

3.3 Universal quantum computation with arbitrary spin measurements

The effect of arbitrary single spin measurements is now considered in general for all $D(Z_d)$ models. The gate set implemented is proved to be universal when d is prime or twice an odd number.

Implementation of controlled-X

Measurement in the basis of spin Pauli operators, as considered in the previous Section, is clearly included within arbitrary spin measurements. As such, certain methods used in the previous section for $D(Z_2)$ can be applied in general for all $D(Z_d)$ models. Notably, using the same circuits as in Fig. 3.2 it is possible to imple-

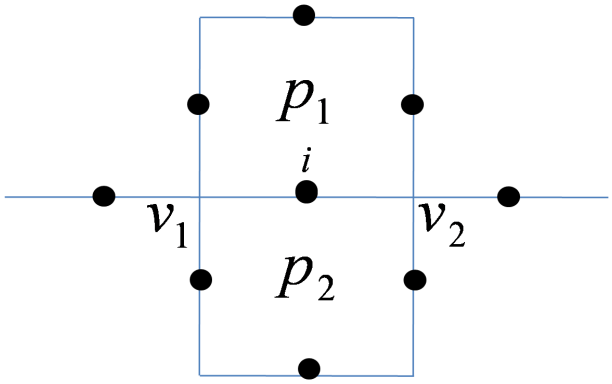

Figure 3.3: Measurements of a single spin affect the surrounding plaquettes and vertices. When a v-type qudit is stored in the two vertices surrounding a spin i, and a p-type in the two plaquettes, measurements of the spin correspond either to measurements of the single qudits, or entangling measurements of the two.

ment the qudit generalization of a controlled-X. This performs an X^g on the target when the control is in state $|\,g\rangle$: $|\,g\rangle\,|\,h\rangle \rightarrow |\,g\rangle\,|\,h+g\rangle$. Again, this is implemented between two v-type qudits, or two p-type qudits. Also, logical Pauli measurements and basis state preparations can be performed using spin Pauli measurements on lattice spins.

Implementation of single spin rotations

It is well known that entangling gates and suitably prepared ancillae can be used to perform single spin rotations [52]. Here we use measurement of lattice spins to prepare logical ancillae that can be used to perform qudit rotations.

Consider any lattice spin i. The two plaquettes and two vertices sharing this spin may be used to define two qudits, one v-type and the other p-type. These are labelled as shown in Fig. 3.3. The vertex v_1 is taken to be that for which i is labelled 1 or 2 and the plaquette p_1 is that for which i is 2 or 3. The logical X operations for these qudits then take the following simple form,

$$X_v = \sigma_i^z, \;\; X_p = \sigma_i^x.$$

A projector acting on spin i can be expressed in terms of the Pauli operators

acting on i and hence, by the relations above, in terms of the logical qudit Pauli operators. Measurements of the spin i therefore correspond to measurements of these qudits. In general these measurements are in an entangled basis of the two qudits. The exceptions are the measurements of σ_i^z and σ_i^x, which correspond to X basis measurements of the v- and p-type qudits, respectively. Note that not all measurements of the two qudits can be achieved in this way, only a certain class.

We consider using these measurements to prepare logical ancilla states. The measurement used is one for which one outcome projects to the state,

$$|\,\phi\rangle_i = \frac{1}{\sqrt{d}} \sum_j e^{i\phi_j} \,|\,j\rangle\,, \tag{3.13}$$

where the ϕ_j are arbitrary and independent phases. The projector onto this state may be expressed,

$$|\,\phi\rangle_i \langle\phi\,| = \frac{1}{d} \sum_{j,k} e^{i(\phi_{j+k}-\phi_j)} \,|\,j+k\rangle_i \langle j\,| = \frac{1}{d^2} \sum_{j,k,l} e^{i(\phi_{j+k}-\phi_j)} \omega^{-jl} X_p^k X_v^l, \tag{3.14}$$

which projects the logical qudits neighbouring the measured spin into the state,

$$|\,\phi\rangle_i \langle\phi\,| \,(|\,0\rangle_p \,|\,0\rangle_v) = \frac{1}{d^2} \sum_{j,k,l} e^{i(\phi_{j+k}-\phi_j)} \omega^{-jl} \,|\,k\rangle_p \,|\,l\rangle_v\,. \tag{3.15}$$

This is a superposition of anyon states on the vertices and plaquettes sharing i, and corresponds to an entangled state of the two logical qudits. However, we are interested only in preparing a single qudit state. To obtain the required state we apply $X_p^\dagger$ to the p qudit and probabilistically project its state onto $|\,0\rangle_p$ using a Z_p measurement. This will leave the v qudit in the state,

$$\frac{1}{\sqrt{d}} \sum_j e^{i(\phi_{j+1}-\phi_j)} \,\big|\,-\tilde{j}\big\rangle_v\,.$$

Application of $F^{\dagger}_{v\to p}$ will then transform this into the p qudit state,

$$\frac{1}{\sqrt{d}}\sum_j e^{i(\phi_{j+1}-\phi_j)}\,|\,j\rangle_p\,.$$

Setting $\phi_0 = 0$ and defining a set of phases θ_k such that $\phi_j = \sum_{k=1\ldots j-1}\theta_k$ for $j = 1\ldots d-1$, this becomes,

$$|\,\theta\rangle_p = \sum_j e^{i\theta_j}\,|\,j\rangle_p\,. \tag{3.16}$$

This is the ancilla state which may be used for single qudit rotations of p-type qudits. It may be prepared for any desired set of θ_k. A corresponding process can be used to prepare the same ancilla state for v-type qudits.

These ancilla states may be used to implement single qudit unitaries of the form,

$$U_z(\theta) = \frac{1}{\sqrt{d}}\sum_j e^{i\theta_j}\,|\,j\rangle\,\langle\,j\,|\,, \tag{3.17}$$

on both v- and p-type qudits. For example, consider a v-type qudit in an arbitrary state $|\,\psi\rangle_v$. Applying the inverse of a controlled-X between this and a logical ancilla in state $|\,\theta\rangle_v$, with the latter as the target, results in the state,

$$\sum_{j,k} e^{i\theta_j}c_k\,|\,k\rangle_v\,|\,j-k\rangle_v = \sum_{j,k} e^{i\theta_{j+k}}c_k\,|\,k\rangle_v\,|\,j\rangle_v\,. \tag{3.18}$$

If the ancilla is then measured in the Z basis and the outcome $j = 0$ obtained, the rotation $U_z(\theta)$ is applied to $|\,\psi\rangle_v$. Otherwise an erroneous rotation occurs. The process may then be repeated until the right result is obtained, changing the θ_j's to correct the erroneous rotations. Each attempt succeeds with a probability of $1/2$, so success can be expected to occur within a small number of steps. The circuit for this process is given in Fig. 3.4. Conjugating $U_z(\theta)$ with the teleporting Fourier transform allows corresponding rotations in the X basis,

$$U_x(\theta) = F^{\dagger}U_x(\theta)F. \tag{3.19}$$

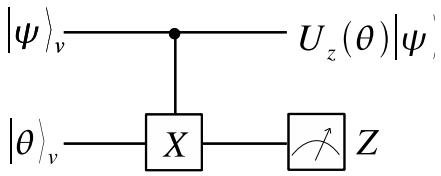

Figure 3.4: The circuit used to implement rotations in the Z basis.

Proof of universality

When d is prime, the single qudit unitaries $U_z(\theta)$ and $U_x(\theta)$ can be used to perform arbitrary single qudit rotations [53]. Along with the entangling controlled-X, this allows for universal quantum computation. Also, as mentioned earlier, the operations that can be implemented in $D(Z_2)$ can also be performed when d is twice an odd number. Hence, since such arbitrary measurements can make $D(Z_2)$ universal, corresponding measurements can also lead to universality in this case. For other cases universality has been neither proved nor disproved.

3.4 Quantum computation without braiding

Certain experimental realizations of Abelian anyons, such as those using Josephson junctions [20], focus on realizing charge anyons at the expense of fluxes, or vice-versa. Only v- or p-type qubits may therefore be encoded, not both, and gates using braiding can no longer be achieved. This applies also to similar partial realizations of non-Abelian models, such as the charges of $D(S_3)$, for which braiding is trivial. It is therefore important to determine what gates it may be possible to utilize to achieve universality in this case, while acting on a minimum number of lattice spins. Here it is shown that acting on a minimum of one spin per logical qubit is sufficient to achieve universality.

In this section we consider a quantum memory based on the charge anyons of Abelian quantum double models, assuming that the plaquettes are always in the vacuum state. This is equivalent to the converse case of using flux anyons in the absence of charges.

Gates without braiding

The encoding defined in Eq. 3.1 is again employed for v-type qudits but, since there can be no flux anyons, no encoding on p-type qudits is possible. This then means that the controlled-Z gate, which is the backbone of all the above, may no longer be used. The logical X and Z may still be used, as their implementation does not necessarily involve braiding. The scheme we consider using these gates also requires measurement of the Z basis, which has been shown above to be possible when lattice spins can be measured in each Pauli basis. However, alternative means to make this measurement would have the same effect.

In order to determine what additional and non-topological gates it might be reasonable to add to the above set, note that the logical X operation acts on a single spin when the two holes are neighbouring. All operations diagonal in the X basis, such as the $U_x(\theta)$ of Eq. 3.19, can therefore also be implemented using single spin operations.

In this same spirit, a two qubit entangling gate diagonal in the X basis of both would act on a minimum of two spins, one for each logical qudit. Such a gate is the the phase-controlled-X: a controlled-X conjugated by the Fourier transform on the source qudit, which implements X^j on the target when the source is in state $\left|\tilde{j}\right\rangle$. Using this, the Fourier transform may be implemented by the circuit of Fig. 3.5.

With the Fourier transform and phase gates $U_x(\theta)$, the phase gates $U_z(\theta)$ may also be performed. As shown above, these can be proven to implement arbitrary single qudit rotations when d is prime, and so universal quantum computation can be performed.

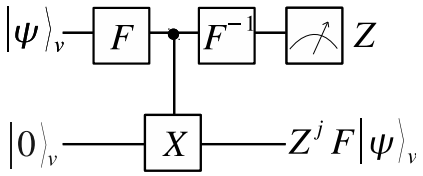

Figure 3.5: The circuit used to implement a Fourier transform, up to a logical Pauli correction, where j denotes the measurement result.

3.5 Conclusions

In this chapter, a range of methods are developed for quantum computation in Abelian quantum double models. These explore the computational power that may be achieved when the different sets of operations are assumed possible. Firstly the use of measurement in the basis of spin Pauli operators was considered. It was shown for the case of $D(Z_{2d_o})$, where d_o is odd, that this allows the implementation of the full Clifford group of gates. The use of arbitrary spin measurements was then considered. This allowed the construction of certain single spin rotations which can be used for universal quantum computation in $D(Z_d)$ models when d is prime, or when $d = 2d_o$.

The chapter is intended to provide a toolkit of methods for quantum computation with Abelian anyons. Though the chapter deals only with quantum double models, many of the techniques may also be applicable for Abelian anyons realized by other means. The results presented here are used in Chapter 6 to determine what proof of principle experiments in topological quantum computation may be performed with current technology. They may also be employed in the advanced encoding of Chapter 5, designed to ensure fault-tolerance.

It is worth mentioning how the results of this chapter compare to the previous work on the topic, as mentioned earlier. The proposal of Dennis et. al [35] treats

the $D(Z_2)$ model simply as a stabilizer code, without consideration of the Hamiltonian. Clifford gates are implemented transversely on logical qubits stored within the stabilizer space. However, the implementation of these requires the system to go via states of superposed anyons. Hence, if a Hamiltonian were to be implemented, these gates would be prone to decoherence. In our proposal the gates are designed to commute with the Hamiltonian, and hence not create excitations. It therefore should not cause decoherence to our logical information, but help to prevent it by providing an energy gap. Such arguments will be applied more rigorously in Chapter 5.

The proposals of Lloyd [36] and Pachos [38], like the one here, store information in such a way that entangling gates may be implemented by braiding. However, unlike here the superpositions of anyon states used for the encoding is degenerate under the Hamiltonian without the need for holes, and can be moved by local potentials. Single qubit rotations are then performed using local gates, which would be implemented by applying local Hamiltonian terms for specific time intervals. As such, they are similar in philosophy to the single qubit rotations of Section 3.4 above. However, in their proposals as well as ours, such gates are susceptible to timing errors. This is in stark contrast to the exact nature of gates implemented by braiding and with well distilled ancilla states [41], such as those in Section 3.3.

Finally, Raussendorf et al. [42] encode logical qubits in holes and implement gates by braiding, supplemented with logical ancillae prepared using single spin measurements. Hence their philosophy is very similar to that used here. However, there are two differences. Firstly, their proposal deals only with $D(Z_2)$, and with a given set of allowed operations. Ours is defined in general for all Abelian quantum double models, and investigates many different sets of operations that may be applicable in different experimental set-ups. Secondly, our proposal is based on Abelian anyons realized on two dimensional spin lattices with a Hamiltonian, whereas theirs is a topologically inspired scheme for measurement based quantum computation. This allows braiding of the holes to be implemented by single spin measurements,

move the holes through simulated time. Even so, the relations between the methods allow the possibility that our work be used in higher dimensional generalizations of their scheme [42].

From these we see the main restriction of the methods proposed in this chapter. Though the means to perform the required braidings were obvious in previous works, it is not clear how this may be done in a practical and fault-tolerant way here. However, this is not a big problem, since this chapter is not intended as a full proposal for quantum computation itself, but as an outline of methods that may be used. These can then be implemented in more advanced encodings in which the means to braid are more straightforward, such as the non-abelian-like encoding of Chapter 5, or generalization of the above schemes to other Abelian models outside the quantum double formalism.

Chapter 4

Simulating non-Abelian anyons with Abelian Models

In this chapter, Abelian anyon models are used to simulate the fusion and braiding behaviour of non-Abelian models. Two examples are considered. The first demonstrates a complete operational equivalence of the Abelian charge anyons of $D(Z_6)$ and the non-Abelian charge anyons of $D(S_3)$. It is shown that there is no detectable difference between the two when restricting to anyonic operations. The second uses the Abelian $D(Z_2)$ model to demonstrate the non-Abelian behaviour of the Ising anyon model, including the non-trivial and chiral nature of the braiding. In both cases, more complex operations than those of the underlying Abelian models must be employed in order for the non-Abelian behaviour to emerge. These include operations which allow superpositions of anyon states to be created and transported coherently, and framings to introduce chirality. For this reason the concept of enhanced Abelian models is developed.

This chapter is structured as follows. Firstly the formalism by which Abelian anyons may be mapped to enhanced Abelian models is introduced in Section 4.1. Then, in Section 4.2, the equivalence of the $D(Z_6)$ and $D(S_3)$ charges is shown. Finally the behaviour of Ising anyons is demonstrated using $D(Z_2)$ in Section 4.3.

4.1 Construction of enhanced Abelian models

The structure of Abelian anyon models is much simpler than that of non-Abelian models. The fusion of Abelian anyons always has a definite result and their F- and R-matrices are all one-dimensional. However, despite this, they are still capable of complex behaviour similar to that found in non-Abelian models.

In order to demonstrate the complex behaviour that may be achieved using Abelian models, an alternate description of them is derived. This redefines the quasiparticles of the model such that fusion and braiding is non-trivial. However, these redefined quasiparticles cannot strictly be described as anyons, so we will not refer to them as such. Instead they will be described simply as quasiparticles of new, enhanced, Abelian models.

Note that an enhanced Abelian model has no physical difference to the Abelian model it is based upon. The difference is only in the way the states are labelled. The non-trivial behaviour realized by the quasiparticles of the enhanced Abelian model is therefore the behaviour of the Abelian anyons, just looked at in a light that illuminates their potential.

Mapping Abelian anyon models to enhanced non-Abelian anyon models

An Abelian model A has a set of N_A particle types, $A = \{1, a, b \ldots\}$. This can be used to define an enhanced Abelian model A' with $N_{A'} < N_A$ particle types, $A' = \{1, \alpha, \beta, \ldots\}$. To do this, the particles of A are decomposed into N_α disjoint sets,

$$A = \{M_1, M_\alpha, M_\beta, \ldots\}. \tag{4.1}$$

All anyons within the set M_α are identified with the quasiparticle α, etc. The set $M_1 = \{1\}$ is defined to contain only the vacuum, so that the vacuum particle of the anyon model is always directly identified with the vacuum of the enhanced Abelian model.

Once the particle types of the enhanced Abelian model have been defined, their fusion rules can be determined. These are directly computed from the fusion rules of the Abelian model by the following relation,

$$N_{\alpha_l,\alpha_m}^{\alpha_n} = \sum_{a_i \in M_{\alpha_l},\, a_j \in M_{\alpha_m},\, a_k \in M_{\alpha_n}} N_{a_i,a_j}^{a_k}. \tag{4.2}$$

The fusion rules of the quasiparticles are determined both by the fusion rules of the underlying anyons and the way in which they are decomposed into sets. Therefore, in general, multiple enhanced Abelian models with different fusion rules can be obtained from the same Abelian model.

These fusion multiplicities demonstrate why the α_n cannot be described as non-Abelian anyons. The abstract theory of anyons is based on the assumption that $N_{\alpha_l,\overline{\alpha}_l}^{1} = 1$, and so a particle and antiparticle fuse to the vacuum in only one distinguishable way. However, as will be seen below when this method is applied, it is possible in enhanced Abelian models to have $N_{\alpha_l,\overline{\alpha}_l}^{1} > 1$. The quasiparticles are therefore not non-Abelian anyons or anyons of any kind.

Transport of the quasiparticles

In order for a physical realization of an Abelian model to support an enhanced Abelian model based upon it, there must exist operations that can map the state of the quasiparticles from one position (a plaquette or vertex, for example) to a neighbouring position. Since, in general, the quasiparticle state may be a superposition of various anyon states, this movement must also be done in a manner that maintains the coherence of the superposition. Furthermore, the operation should be quasi-local, acting only in the neighbourhood of the positions moved from and to.

For any enhanced Abelian model, a transport protocol can be designed in a way similar to the transport of non-Abelian anyons in [24]. Though our focus is on quantum double models realized on spin lattices, we present the protocol in a general way that should be applicable to all Abelian models, regardless of the physical medium used to realize them.

Given a physical realization of an Abelian anyon model, let us use $t_{x,x'}(a_n)$ to denote the operation to move an anyon a_n to from a position x to x' and $P_x(a_n)$ to denote the projector onto the state of an anyon of type a_n present at x. To move a quasiparticle α_m from x to x' we first take an ancillary $|M_{\alpha_m}|$-level spin q whose basis states are denoted $|\, n\rangle_q$ for each $a_n \in M_{\alpha_m}$. This is initially prepared in some known initial state $|\, \theta\rangle_q$. The following unitary operation can then be performed between the physical medium used to realize the anyons and the ancilla,

$$C_x(\alpha_m) = \sum_{a_n \in M\alpha_m} P_x(a_n) \otimes |\, n\rangle \langle \theta \,| + \text{other terms.} \tag{4.3}$$

The other terms mentioned here are required for unitarity, but only relevant when the ancilla is in an initial state other than $|\, \theta\rangle$. However, since we do not consider such cases, we need not consider these terms. The operation entangles the ancilla to the anyon occupation state at position x: when an a_n is present at x the ancilla is mapped to state n. The following unitary may then be applied,

$$D_{x'}(\alpha_m) = \sum_{a_n \in M\alpha_m} t_{x,x'}(a_n) \otimes |\, n\rangle \langle n \,| \,. \tag{4.4}$$

This applies an operation $t_{x,x'}(a_n)$ to the physical medium according to the state of the ancilla. This ensures that the correct operation is applied to move the anyon present. Finally the operation $C^\dagger_{x'}(\alpha_m)$ is applied. If the position x' was previously unoccupied, this disentangles the ancilla and returns it to its initial state $|\, \theta\rangle$. If the position was occupied by some other quasiparticle α_l, the state of the ancilla will, in general, remain entangled. Measurement of its state will reveal the channel of the fusion $\alpha_m \times \alpha_l$.

In any case, the application of the operations above results in the transport of the quasiparticle which, when an ancilla located close to x and x' is used, is quasilocal. Furthermore, when these operations are used to fuse and braid the underlying anyons, the same fusion and braiding behaviour is obtained as would be expected from the model.

4.2 Realizing $D(S_3)$ charges with $D(Z_6)$

Introduction

Using enhanced Abelian models, it can be shown that the non-Abelian charge anyons of the $D(S_3)$ model are equivalent in behaviour to the Abelian charge anyons of the $D(Z_6)$ model. Applying the operations of creation and transport of $D(S_3)$ charges yields the same fusion results as the quasiparticles of an enhanced Abelian model.

This equivalence only applies to a certain extent. There will be multiplicities present in the fusion rules of the quasiparticles of the enhanced Abelian model not present in the anyons, and relative phases in the F-matrices of the anyons not realized by the quasiparticles. However, so long as only the operations of creation and transport, and measurements of fusion results are used, these differences cannot be detected.

The $D(Z_6)$ model

The $D(Z_6)$ model is an Abelian quantum double model, with charge, flux and composite anyons. The model has a spin lattice realization, as discussed earlier (2.2), but this need not be considered here. As in all Abelian quantum double models, the charge and flux anyons are the exact mirror of each other. Either can therefore be shown to be equivalent to the charges of $D(S_3)$, but the charges are chosen for the sake of later discussions of experimental realizations in Chapter 6. The properties of these charge anyons are as follows.

- *Particle types:*

$$e^0,\ e^1,\ e^2,\ e^3,\ e^4,\ e^5. \tag{4.5}$$

  The e^0 charge anyon is identified with the vacuum, 1.

- *Fusion rules:*

$$e^g \times e^h = e^{g+h \bmod 6},\ \forall\ g, h \in Z_6. \tag{4.6}$$

- *R-matrices:* All trivial.

- *F-matrices:* All trivial.

The charge submodel of $D(S_3)$

The charge submodel of $D(S_3)$ was presented in detail in Section 2.3. The non-Abelian braiding of this model is only sufficient to represent the permutation of the anyons, and does not perform any additional operations on the fusion space. It is this property that allows these non-Abelian anyons to be made equivalent to Abelian anyons in a straightforward manner.

An enhanced Abelian model of $D(Z_6)$

Consider the following enhanced Abelian model of the $D(Z_6)$ charges,

$$M_1 = \{e^0\},\ M_{\tilde{\Phi}} = \{e^1, e^2, e^4, e^5\},\ M_{\tilde{\Lambda}} = \{e^3\}. \tag{4.7}$$

This leads to the fusion rules,

$$\tilde{\Phi} \times \tilde{\Phi} = 4 \cdot 1 + 4 \cdot \tilde{\Lambda} + 8 \cdot \tilde{\Phi}, \quad \tilde{\Lambda} \times \tilde{\Lambda} = 1, \quad \tilde{\Phi} \times \tilde{\Lambda} = 4 \cdot \tilde{\Phi}, \tag{4.8}$$

which, aside from the multiplicities, are the same as those of the $D(S_3)$ charges (Eq. 2.21).

The states of $\tilde{\Phi}$ quasiparticles

The $\tilde{\Phi}$ quasiparticles are defined as being any anyon from the set $M_{\tilde{\Phi}}$. The state of a single $\tilde{\Phi}$ residing at some position n can therefore be any arbitrary mixture of these anyon states,

$$\rho_{\tilde{\Phi}_n} = c_1 \left| e_n^1 \right\rangle \left\langle e_n^1 \right| + c_2 \left| e_n^2 \right\rangle \left\langle e_n^2 \right| + c_4 \left| e_n^4 \right\rangle \left\langle e_n^4 \right| + c_5 \left| e_n^5 \right\rangle \left\langle e_n^5 \right|). \tag{4.9}$$

Here the n subscript, for both the $\tilde{\Phi}$ and e^g, denotes the position of the quasiparticles. The reason why the state of the single $\tilde{\Phi}$ must be a mixture is that the superposition

of anyons of different states is impossible, only the superposition of states of the same total fusion channel forms a physical state. Hence, for example, a pair of $\tilde{\Phi}$ quasiparticles that belong to the vacuum sector can be an arbitrary superposition of any such pairs of the anyons in $M_{\tilde{\Phi}}$,

$$\left| \tilde{\Phi}_n, \tilde{\Phi}_m; 1 \right\rangle = a_1 \left| e_n^1, e_m^5 \right\rangle + a_2 \left| e_n^2, e_m^4 \right\rangle + a_4 \left| e_n^4, e_m^2 \right\rangle + a_5 \left| e_n^5, e_m^1 \right\rangle . \tag{4.10}$$

In the following the exact forms of these states must be determined in order to satisfy the fusion rules.

Equivalence of fusion behaviour

We will first consider the equivalence of fusion behaviour in the two models. We have seen that the fusion rules differ only in the values of the multiplicities, so it only remains to show that the F-matrices are satisfied. Since only measurements of anyons are considered, relative phases between anyon states cannot be detected. Only the probabilities for fusion outcomes predicted by the F-matrices must therefore be reproduced. The only non-trivial F-matrix for the $D(S_3)$ charges corresponds to the case where three Φ charges fuse to a Φ. Let us suppose that these anyons are located at positions denoted 1, 2 and 3, and so can be labelled Φ_1, Φ_2 and Φ_3 accordingly. When the anyons are prepared in a state such that Φ_1 and Φ_2, if fused, would fuse to the result $a \in \{1, \Phi, \Lambda\}$, the probability that Φ_2 and Φ_3 will fuse to $b \in \{1, \Phi, \Lambda\}$ is,

$$P(b|a) = |(F^{\Phi}_{\Phi\Phi\Phi})^b_a|^2. \tag{4.11}$$

This follows from the definition of the F-matrix in 2.1. From Eq. 2.23, these probabilities are,

$$\begin{aligned} P(1|1) = 1/4,\ P(\Lambda|1) &= 1/4,\ P(\Phi|1) = 1/2, \\ P(1|\Lambda) = 1/4,\ P(\Lambda|\Lambda) &= 1/4,\ P(\Phi|\Lambda) = 1/2, \\ P(1|\Phi) = 1/2,\ P(\Lambda|\Phi) &= 1/2,\ P(\Phi|\Phi) = 0. \end{aligned}$$

In order to reproduce the probabilities, the states of any $\tilde{\Phi}$ quasiparticle must be an equally weighted mixture of all the anyons in $M_{\tilde{\Phi}}$,

$$\rho_{\tilde{\Phi}_n} = \frac{1}{4}(|\, e_n^1\rangle\langle e_n^1\,| + |\, e_n^2\rangle\langle e_n^2\,| + |\, e_n^4\rangle\langle e_n^4\,| + |\, e_n^5\rangle\langle e_n^5\,|). \tag{4.12}$$

Accordingly, the state of $\tilde{\Phi}$ pairs in the vacuum and $\tilde{\Lambda}$ fusion channels is defined to be,

$$\begin{aligned} \left|\tilde{\Phi}_1, \tilde{\Phi}_2; 1\right\rangle &= \frac{1}{2}(|\, e_1^1, e_2^5\rangle + |\, e_1^5, e_2^1\rangle + |\, e_1^2, e_2^4\rangle + |\, e_1^4, e_2^2\rangle) \\ \left|\tilde{\Phi}_1, \tilde{\Phi}_2; \tilde{\Lambda}\right\rangle &= \frac{1}{2}(|\, e_1^1, e_2^2\rangle + |\, e_1^2, e_2^1\rangle + |\, e_1^4, e_2^5\rangle + |\, e_1^5, e_2^4\rangle). \end{aligned} \tag{4.13}$$

Introducing an external Φ_3 and fusing it with Φ_2 will then correspond to an equally weighted mixture of sixteen anyon fusions. Four of these yield the vacuum, four yield a $\tilde{\Lambda}$ and eight yield a $\tilde{\Phi}$, hence giving the correct probabilities for each.

The third fusion process to be considered is that of three $\tilde{\Phi}$'s, in a state for which $\tilde{\Phi}_1 \times \tilde{\Phi}_2 = \tilde{\Phi}$ and $\tilde{\Phi}_1 \times \tilde{\Phi}_2 \times \tilde{\Phi}_3 = \tilde{\Phi}$. In terms of the anyons, the states which satisfy these take one of the following two forms,

$$\left|e_1^{1+i}, e_1^{1+j}, e_1^{2+k}\right\rangle, \left|e_1^{2+i}, e_1^{2+j}, e_1^{1+k}\right\rangle, \; i,j,k \in \{0,3\}. \tag{4.14}$$

From these, it is easy to see that $\tilde{\Phi}_2 \times \tilde{\Phi}_3$ can only be 1 or $\tilde{\Lambda}$, reproducing the required probability $P(\Phi|\Phi) = 0$. Defining $\tilde{\Phi}$'s to satisfy Eq. 4.12 ensure that neither the 1 or $\tilde{\Lambda}$ is preferred, so $P(1|\Phi) = P(\Lambda|\Phi) = 1/2$, as required.

Since these states do not simply correspond to those of the underlying anyons, but superpositions of them, they cannot be prepared using the same simple creation operators. Instead, more complex operations must be employed. It is the use of these, along with the quasiparticle transport operations outlined previously, that allow non-Abelian behaviour to emerge from this Abelian model.

Equivalence of braiding behaviour

The abstract theory of anyons as presented in 2.1 treats anyons of the same type as indistinguishable. Therefore, the effect of their permutation must be represented in the braid matrices. In a physical realization of anyons on a spin lattice, however, the quasiparticles are distinct entities in the lattice. Their permutation is therefore represented by simply taking the quasiparticles and exchanging them. Hence the effect of the braid matrix is realized, even if the exact phase factors it specifies cannot be seen to have been realized explicitly.

In the case of the $D(S_3)$ anyons the $R^{\Phi\Phi}$ matrix has one non trivial entry, $R^{\Phi\Phi}_{\Lambda} = -1$, which states that a phase of -1 should result when two Φ's of the Λ fusion channel are exchanged. Though such a phase cannot be seen to result from the exchange of the $\tilde{\Phi}$ quasiparticles, its effect on the fusion outcomes is achieved when they are moved around each other. Hence the effect of the R-matrix is fully realized. This is exactly the same way as the R-matrix is reproduced in for the Φ anyon in the actual $D(S_3)$ lattice model.

With both braiding and fusion shown to be equivalent, the $\tilde{\Phi}$ and $\tilde{\Lambda}$ quasiparticles will always yield the same results with the same probabilities as the charge submodel of $D(S_3)$. The two may therefore be considered to be completely operational equivalent when only the anyonic operations of braiding and fusion are performed. This allows experiments to be designed which could realize these anyons in a simpler manner than usually expected for non-Abelian anyons, as will be discussed later in Chapter 6.

Uses of the simulation

In the above it was shown that an enhanced $D(Z_6)$ model, in which superpositions of the charge anyons can be created and manipulated, is equivalent to the charge submodel of $D(S_3)$ when only operations of fusion and braiding are considered. However, it should be noted that the superpositions are not actually required in order to satisfy this equivalence, since statistical mixtures will also suffice. One

might therefore question whether this is truly a realization of non-Abelian anyons.

As discussed in Section 2.1 of Chapter 2, all realizations of anyons are simulations with certain limits. The limits for this simulation of the $D(S_3)$ are that only the anyonic operations of braiding and fusion may be implemented. The effects of other, non-topological operations, would not be expected to yield the same results as predicted by the anyonic theory.

The limitations of this simulation, coupled with the simplicity of the model simulated, means that the anyonic behaviour realized by the above could not be harnessed for fault-tolerant quantum computation. This point is underlined by the fact that the superposition states used in the above could be replaced by statistical mixtures, without making any difference to the results. The simulation therefore has no need to maintain to coherence of the states, and could not be used as a quantum memory. This primary use of this simulation is therefore as a first step toward more complex realizations of anyonic behaviour. It provides a testing ground in which the spin lattice models may be constructed and quasiparticles may be created and manipulated without stringent requirements on the coherence of states.

4.3 Realizing Ising anyons with $D(Z_2)$

Introduction

In the previous Section an Abelian anyon model, supplemented by additional operations, was shown to realize the same behaviour as a non-Abelian model. This was facilitated by the simple braiding behaviour of the non-Abelian model in question. Now it will be demonstrated that an Abelian model can also demonstrate the behaviour of a non-Abelian model whose braiding is not trivial, but which implements rotations in the fusion space. This will require a more careful approach to the fusion multiplicities of the enhanced Abelian model used, which must be eliminated for consistency.

The Abelian model used is the $D(Z_2)$ quantum double model, well known as the

anyon model of the toric code. This is shown to realize the braiding and fusion behaviour of the non-Abelian Ising anyon model. Chirality is introduced using framing, which brings about the correct phase factors to accompany the exchange statistics.

Though the Ising anyon model is known to exist in a phase of the honeycomb lattice model [51, 55], it does not have a well known spin lattice realization. It is still an open question as to how the anyons are created and transported by spin operations, and how these lead to the braid relations. Our simulation of the properties of this model in a well understood spin lattice realization sheds light on this problem, especially since the $D(Z_2)$ model is also a phase of the honeycomb lattice model.

The $D(Z_2)$ anyon model

The $D(Z_2)$ anyon model is the simplest and most well understood of all Abelian models. It is the anyon model of the toric code, and related surface codes [34, 35]. This makes it the most well known anyon model both inside and outside the community of topological quantum computation. Its properties are as follows.

- *Particle types:*

$$1,\ e,\ m,\ \epsilon. \tag{4.15}$$

- *Fusion rules:*

$$e \times e = m \times m = \epsilon \times \epsilon = 1,\ e \times m = \epsilon,\ e \times \epsilon = m,\ m \times \epsilon = e.$$

- *R-matrices:*

$$R_1^{\epsilon\epsilon} = (R_\epsilon^{em})^2 = -1,\ R_1^{ee} = R_1^{mm} = 1,$$

- *F-matrices:* All trivial.

The spin lattice model usually used to realize the $D(Z_2)$ model is a square lattice with a spin-1/2 particle on each edge [34]. Instead we consider a hexagonal lattice

with spins on the vertices. These two descriptions are equivalent, as shown in Fig. 4.1. Each plaquette P is split into two subplaquettes, labelled s to the left and p to the right. The following operators are then defined on the four spins around each subplaquette,

$$A_s = \sigma_1^x \sigma_2^x \sigma_3^x \sigma_4^x, \; B_p = \sigma_1^z \sigma_2^z \sigma_3^z \sigma_4^z. \tag{4.16}$$

The anyon vacuum is associated with any state for which $A_s \,|\, \xi\rangle = |\, \xi\rangle$ and $B_p \,|\, \xi\rangle = |\, \xi\rangle$ for all s and p. Any state for which $A_s \,|\, e_s\rangle = -\,|\, e_s\rangle$ is identified with an e anyon located at the subplaquette s. Similarly $B_p \,|\, m_p\rangle = -\,|\, m_p\rangle$ is identified with an m anyon at p. An ϵ is present on a plaquette P if both an e and an m anyon are present on the corresponding subplaquettes. This is due to the fusion rule $e \times m = \epsilon$.

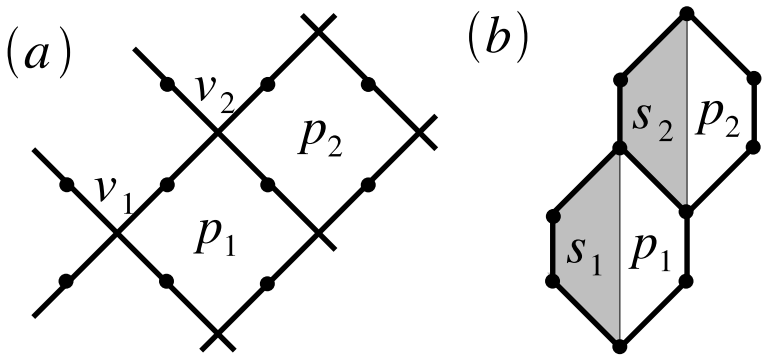

Figure 4.1: The same spins are depicted in (a) on the edges of a square lattice and in (b) on the vertices of a hexagonal lattice. The vertices v_1 and v_2 in the former correspond to subplaquettes s_1 and s_2 in the latter, respectively. The plaquettes p_1 and p_2 also correspond to subplaquettes with the same labels.

The Ising anyon model

The Ising anyon model was presented in detail in 2.4. It is one is one of the simplest non-Abelian models which, unlike the charge submodel of $D(S_3)$ above, has braiding which acts non-trivially on the fusion space. In fact, its braiding is sufficient to realize the Clifford group of gates on logical qubits stored within the fusion space

[41]. though it is known that the Ising anyon model emerges in a certain coupling regime of the honeycomb lattice model, as discussed in 2.4, an explicit understanding of how the anyons are realized in terms of the underlying spins is not known. Any insight into how this may work is then valuable to current research in the field.

The enhanced Abelian model of $D(Z_2)$

In order to demonstrate the behaviour of the Ising anyon model, we map the Abelian anyon model of $D(Z_2)$ into an enhanced Abelian model as follows,

$$A_{D(Z_2)} = \{1, e, m, \epsilon\} = \{M_1, M_{\tilde{\sigma}}, M_{\tilde{\psi}}\},\ M_1 = \{1\},\ M_{\tilde{\sigma}} = \{e, m\},\ M_{\tilde{\psi}} = \{\epsilon\}. \quad (4.17)$$

With this decomposition we directly identify the vacuum and ϵ of the anyon model with the vacuum and $\tilde{\psi}$ of the enhanced Abelian model, respectively. The e and m are then both identified with the $\tilde{\sigma}$.

Equivalence of fusion behaviour

With the above decomposition of the $D(Z_2)$ anyons, the fusion rules are,

$$\tilde{\sigma} \times \tilde{\sigma} = 2 \cdot 1 + 2 \cdot \tilde{\psi}, \quad \tilde{\psi} \times \tilde{\psi} = 1, \quad \tilde{\sigma} \times \tilde{\psi} = 2 \cdot \tilde{\sigma}. \quad (4.18)$$

Aside from the multiplicities, these take the same form as the fusion rules for the Ising anyon model (Eq. 2.27). In order to eliminate these multiplicities, and faithfully replicate the Ising anyon model fusion rules, we must place restrictions on the states of quasiparticles that may be used in the enhanced Abelian model.

Consider a pair of $\tilde{\sigma}$ quasiparticles located at plaquettes P_1 and P_2. These are denoted $\tilde{\sigma}_1$ and $\tilde{\sigma}_2$, respectively. The possible states for a pair in the vacuum fusion channel are,

$$|\,\tilde{\sigma}_1, \tilde{\sigma}_2\rangle = \alpha\,|\,e_1, e_2\rangle + \beta\,|\,m_1, m_2\rangle\,, \quad (4.19)$$

For a pair in the $\tilde{\psi}$ fusion channel,

$$|\,\tilde{\sigma}_1, \tilde{\sigma}_2\rangle = \alpha\,|\,e_1, m_2\rangle + \beta\,|\,m_1, e_2\rangle\,. \tag{4.20}$$

From these it can be seen that a two dimensional space is associated with each fusion outcome, leading to the multiplicity of 2 for each. However, we will restrict to just the two states, depicted in Fig. 4.2,

$$|\,\tilde{\sigma}_1, \tilde{\sigma}_2; j\rangle = \frac{1}{\sqrt{2}}(|\,e_1, e_2\rangle + j\,|\,m_1, m_2\rangle), \tag{4.21}$$

for $j = \pm 1$. Both of these states are of the vacuum fusion channel, leading to the fusion rule $\tilde{\sigma} \times \tilde{\sigma} = 2 \cdot 1$. However we will identify the $j = -1$ state with the $\tilde{\psi}$ fusion channel. The quasiparticle $\tilde{\psi}$ is then no longer simply identified with the ϵ of the $D(Z_2)$ model, but also this state of a $\tilde{\sigma}$ pair. The fusion rule then becomes $\tilde{\sigma} \times \tilde{\sigma} = 1 + \tilde{\psi}$, just as in the Ising anyon model. Note that these two states are locally indistinguishable, since the $\tilde{\sigma}$ is an equal mixture of e and m in either state. Also fusion with a $\tilde{\psi}$ does not change the $\tilde{\sigma}$ in any way that can be detected locally. This is what one would expect from a fusion channel of anyons. Also, it means that there is no longer a multiplicity in this fusion, so $\tilde{\sigma} \times \tilde{\psi} = \tilde{\sigma}$.

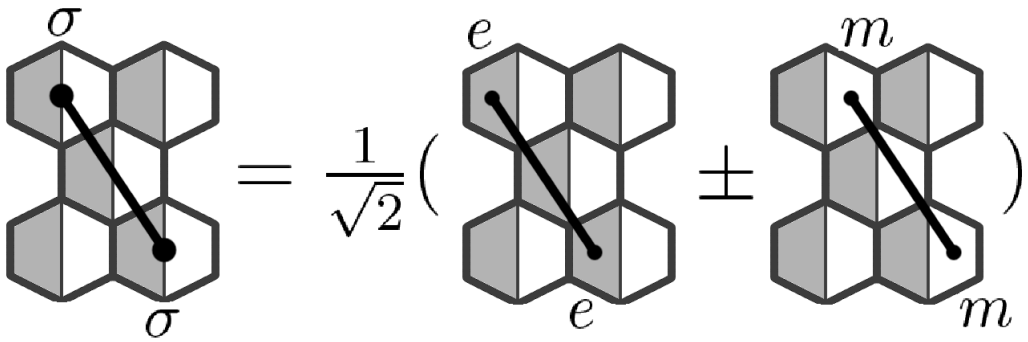

Figure 4.2: The state of a σ pair with endpoints in two plaquettes of the honeycomb lattice can be described by a superposition of e and m pair. The relative $\pm$ sign is a non-local property that cannot be accessed by measurements at either endpoint.

Now we have determined the conditions under which the the correct fusion rules

are realized, it remains to demonstrate that the F-matrices are obeyed. Since restrictions have been placed on the possible states for $\tilde{\sigma}$ pairs, corresponding restrictions must also be placed on allowed fusion processes so that only allowed states emerge. In addition, since we treat the vacuum channel $j = -1$ state as a $\tilde{\psi}$ channel state, we must be careful which fusions we allow it to undergo. After these considerations, the set of allowed fusions is found to be those in which pairs of anyons are fused to yield other pairs.

To clarify this point, consider two pairs of σ anyons, both in the vacuum fusion channel. The collective state of the four anyons is therefore also in the vacuum channel. We use σ_1 and σ_2 to denote the anyons of the first pair, and σ_3 and σ_4 to denote those of the second. We define the fusion of these pairs to be the fusion of σ_1 with σ_3 and σ_2 with σ_4. Since these collectively belong to the vacuum channel, both fusions will yield either the vacuum, and hence a vacuum pair, or both will yield a ψ, and hence a ψ pair. The general case is depicted in Fig. 4.3.

The allowed fusions are then:

- The fusion of two $\tilde{\sigma}$ pairs, both of the vacuum fusion channel.
- The fusion of two $\tilde{\sigma}$ pairs, both of the $\tilde{\psi}$ fusion channel.
- The fusion of a $\tilde{\psi}$ pair with any $\tilde{\sigma}$ pair.
- The fusion of two $\tilde{\psi}$ pairs.

The only non-trivial F-matrix for us to consider is that for σ anyons (Eq. 2.29), which affects the fusion in Fig. 4.3. In order to satisfy this, the fusion of two $\tilde{\sigma}$ pairs must yield an equally weighted superposition of a vacuum pair and a $\tilde{\psi}$ pair. When both $\tilde{\sigma}$ pairs are of the vacuum fusion channel, this superposition has a relative phase of $+1$. On the other hand, when they are of the $\tilde{\psi}$ channel the phase is -1.

The state of two pairs, either both in the vacuum channel ($j = +1$) or both in

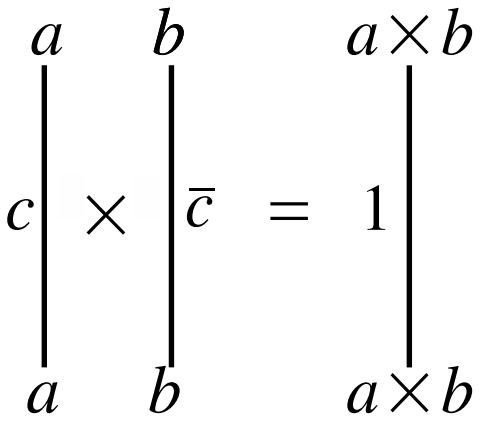

Figure 4.3: A pair of a anyons of the c fusion channel and a pair of b anyons of the $\bar{c}$ fusion channel are depicted. The fusion of these pairs corresponds to the fusion of each a with a b. This yields a pair of $a \times b$ anyons of the vacuum fusion channel.

the $\tilde{\psi}$ channel ($j = -1$), is as follows.

$$\begin{aligned}
|\,\sigma_1,\sigma_2;+1\rangle\,|\,\sigma_1,\sigma_2;+1\rangle &= \frac{1}{2}(|\,e_1,e_2,e_3,e_4\rangle + |\,m_1,m_2,m_3,m_4\rangle \\
&+ |\,e_1,e_2,m_3,m_4\rangle + |\,m_1,m_2,e_3,e_4\rangle), \\
|\,\sigma_1,\sigma_2;+1\rangle\,|\,\sigma_1,\sigma_2;+1\rangle &= \frac{1}{2}(|\,e_1,e_2,e_3,e_4\rangle + |\,m_1,m_2,m_3,m_4\rangle \\
&- |\,e_1,e_2,m_3,m_4\rangle - |\,m_1,m_2,e_3,e_4\rangle). \qquad (4.22)
\end{aligned}$$

Let us consider the fusion of these pairs by fusing the contents of plaquette P_1 with that of P_3, and that of P_2 with that of P_4. In the first two terms of each of the above states these fusions yield the vacuum, and in the latter two they yield a $\tilde{\psi}$, so we denote them

$$\begin{aligned}
|\,1_{1,3},1_{2,4}\rangle &= \frac{1}{\sqrt{2}}(|\,e_1,e_2,e_3,e_4\rangle + |\,m_1,m_2,m_3,m_4\rangle), \\
|\,\psi_{1,3}\psi_{2,4}\rangle &= \frac{1}{\sqrt{2}}(|\,e_1,e_2,m_3,m_4\rangle + |\,m_1,m_2,e_3,e_4\rangle). \qquad (4.23)
\end{aligned}$$

The states of two pairs may then be written

$$\begin{aligned} |\,(\sigma_1,\sigma_2;+1)(\sigma_3,\sigma_4;+1)\rangle &= \frac{1}{\sqrt{2}}(|\,1_{1,3},1_{2,4}\rangle + |\,\psi_{1,3}\psi_{2,4}\rangle), \\ |\,(\sigma_1,\sigma_2;-1)(\sigma_3,\sigma_4;-1)\rangle &= \frac{1}{\sqrt{2}}(|\,1_{1,3},1_{2,4}\rangle - |\,\psi_{1,3}\psi_{2,4}\rangle). \end{aligned} \tag{4.24}$$

Here we see that these fusions yield the superposition and relative sign in exactly the way predicted by the F-matrix. The $\tilde{\sigma}$ and $\tilde{\psi}$ quasiparticles of $D(Z_2)$ therefore reproduce the fusion behaviour of the σ and ψ anyons of the Ising anyon model for the restricted set of fusions considered.

Equivalence of braiding behaviour

By considering the decompositions of the $\tilde{\sigma}$ and $\tilde{\psi}$ particles in terms of the $D(Z_2)$ particles we can show that they satisfy the Ising anyon model braiding rules. For example, let us consider the exchange of two $\tilde{\psi}$'s. Since these are identified with the ϵ's of $D(Z_2)$ they will have the same fermionic behaviour. Also, since the braiding of an e or an m around an ϵ results in a phase factor of -1, so does the braiding of a $\tilde{\sigma}$ around a $\tilde{\psi}$. Let us also consider the braiding of two of the $\tilde{\sigma}$ particles, such as those in Eq. 4.22. Braiding the $\tilde{\sigma}$ residing at plaquette 1 around that at 3 results in a change of the relative sign for both $\tilde{\sigma}$ pairs, and so a change also of the relative sign between the vacuum and fermion pairs in the fusion outcome. From this we infer the R matrices $(R_1^{\sigma\sigma})^2 = 1$ and $(R_\psi^{\sigma\sigma})^2 = -1$. These are similar to those of the Ising anyon model, except that a complex phase factor is missing. This required phase differs for anticlockwise and clockwise braidings, $e^{-i\pi/4}$ for the former and $e^{i\pi/4}$ for the latter. Since $R = R^\dagger$ for the toric code particles, the lattice does not distinguish between anticlockwise and clockwise evolutions. A framing [12] is therefore proposed for the σ particles to make this distinction and to encode the chirality on an ancillary system.

We allocate two framings to each $\tilde{\sigma}$ particle, one to the left (l) and one to the right (r). Each of them has an ancillary qubit, initially in the zero state, $|\,0\rangle_l\,|\,0\rangle_r$.

When the particle moves the framings move with it, performing the operation

$$E_i = |+\rangle\langle+| \otimes 1_i \quad + \quad |-\rangle\langle-| \otimes (i\sigma_i^y). \tag{4.25}$$

between their ancillary qubits and the lattice sites, i, to the left and right of the particle. This creates superpositions of the vacuum and an ϵ, controlled on the ancilla state. When the loops are complete the framings act trivially on the lattice, but may cause a bit flip on the ancilla depending on whether the ϵ loop acquired a -1 by braiding around a $\tilde{\sigma}$ string. After each loop the ancillary qubits are measured and the operations $e^{i\pi/8}\sigma_r^x$ and $e^{-i\pi/8}\sigma_l^x$ applied for the results $|0\rangle_l|1\rangle_r$ and $|1\rangle_l|0\rangle_r$ respectively. These assign a phase and reset the qubits. The state $|0\rangle_l|1\rangle_r$, for example, is assigned $e^{i\pi/8}$ since it is the result of either an anticlockwise loop that encloses no other $\tilde{\sigma}$ particle or a clockwise loop which does enclose a $\tilde{\sigma}$ particle. In the former case this phase comes from the fact that the loop causes the extended object of the $\tilde{\sigma}$ particle and framing to undergo a anticlockwise twist of 2π. This must therefore be assigned the phase $e^{i\pi/8}$, due to a topological spin. In the latter case the phase comes from both a clockwise braiding and a twist, $e^{i\pi/4}e^{-i\pi/8} = e^{i\pi/8}$. The consistency of this framing can be verified in Fig. 4.4, where a complete set of elementary cases have been considered.

The phase factor required for the R matrix is that for a braiding in which a σ particle performs a loop around another particle without twisting. So the twists must be removed from the above loops in order to obtain the corresponding evolutions. This can be done by following all loops with a twist alone in the opposite direction. By this two stage process the framing applies the required phase of $e^{-i\pi/4}$ for an anticlockwise braiding. When the phase is inserted it gives the R matrix required for the consistency of the Ising anyon model.

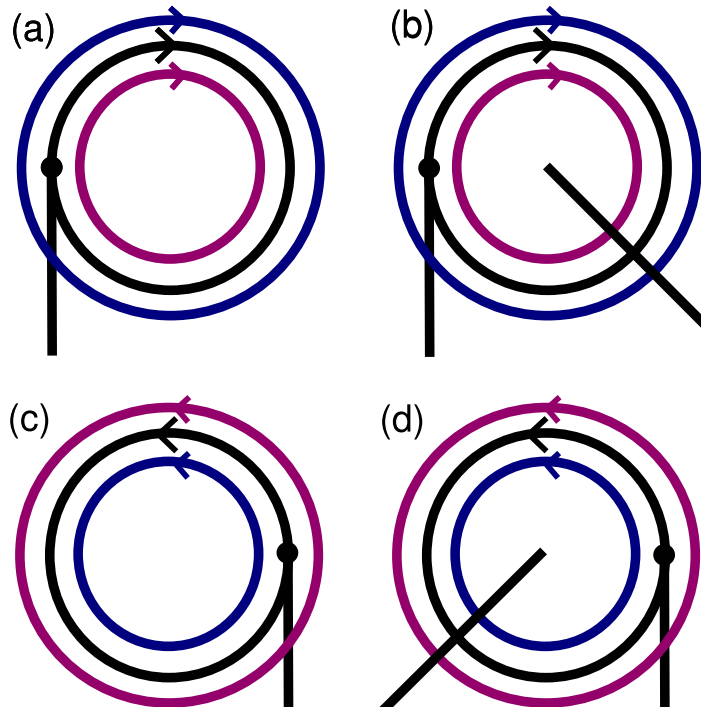

Figure 4.4: The four possible loops for a $\tilde{\sigma}$ particle that start and finish at the marked points, where the framing is depicted. The loops to the top are clockwise and those to the bottom are anti-clockwise . The loops to the left enclose no other $\tilde{\sigma}$ particle and those to the right do. In (a) and (d) the left framing braids around a $\tilde{\sigma}$ string once and the right framing does not braid or braids twice, resulting in a bit flip on the ancillary qubit for the left framing only. In (b) and (c) the situation is reversed.

Redefined plaquette operators

Consider the plaquette operators,

$$W_P = A_s B_p, \;\; W'_P = \frac{1}{2}(1 + A_s + B_p - A_s B_p), \tag{4.26}$$

on the plaquettes of the honeycomb lattice, where s and p are the subplaquettes of P. The operator W_P detects whether an e or an m is present on P without distinguishing between the two. It is therefore well suited to the $\tilde{\sigma}$ quasiparticle, since it can detect these without collapsing or otherwise changing the superposition. It also bears a striking resemblance to the operator that detects the σ anyons in Kitaev's honeycomb lattice model, as described in Section 2.4. The operator W'_P

detects the state of the plaquette in which both an e and an m is present, and is therefore well suited to the $\tilde{\phi}$ quasiparticle.

4.4 Conclusions

Here we introduced the idea that Abelian anyon models, when properly supplemented with additional operations, can realize some of the behaviour of non-Abelian anyons. This is a new method of building spin lattice representations anyons in which complex models are engineered from simpler ones. Though the methods employed here were applied to quantum double models, it is expected to be applicable to all anyons realized on spin lattices [12, 13]. Many of the techniques may also be applicable in the case of the fractional quantum Hall effect, though this would require further study.

This study leads to several important theoretical insights. It sheds light on the way in which non-Abelian behaviour can be realized in spin lattices. This paves the way for an understanding of models, such as the Ising anyon model, whose spin level description is beyond the stabilizer formalism. It could therefore aid the description of the non-Abelian phase Kitaev's honeycomb lattice model at the spin level [51].

These models also show how important it is to determine the limitations of any simulation of anyons. No experimental demonstration of anyons should be considered complete without a full appraisal of what aspects of anyonic behaviour it can and cannot reproduce, and the restrictions on what operations may be performed in order to do this. Only this will distinguish those simulations that reproduce anyonic operations completely without being able to form a stable quantum memory, like that of Section 4.2, from those that can be harnessed for fault-tolerant quantum computation. Such an appraisal would ideally be made by applying a universal set of gates on the fusion space, to determine whether this has the effects predicted by anyonic theory. Also, Bell's inequalities may also be considered using the anyon states, the ensure that the anyonic behaviour truly emerges from quantum effects [43].

This work also gives insight into the study of multipartite entanglement, especially the so-called topological entanglement. It is known that the realization of anyonic quasiparticles requires physical mediums which exhibit topological entan-

glement. The amount of this entanglement, as defined by the topological entropy, is related to the total quantum dimension of the model. Models with the same total quantum dimension are therefore supported by entangled states with the same topological entanglement entropy. However, nothing was known about how these states relate to each other; whether they belong to the same entanglement class, or whether they are inequivalent. This is especially true if the anyon models have markedly different properties. In the above we have proved equivalences between the charge submodels of $D(Z_6)$ and $D(S_3)$, which both have total quantum dimension of $\sqrt{6}$, and between $D(Z_2)$ and the Ising anyon model, both with a total quantum dimension of 2. This demonstrates that states capable of supporting models with a given value of D can, in some cases at least, support other models with the same value even, when one is Abelian and the other non Abelian, or when one is chiral and the other is not. It is worth noting that a similar result emerges fron Kitaev's honeycomb lattice mode [51], for which three anyon models can be realized in different phases, all with the same total quantum dimension [57]. This provides another means by which the relationship between topologically entangled states may be studied.

The findings of this chapter also have important consequences experimentally. The relative simplicity of Abelian anyons has lead to their demonstration in the laboratory, and further progress is always being made. The fact that these anyons can be used to realize the behaviour of their non-Abelian counterparts then brings the experimental realization of non-Abelian anyons even closer. This is discussed further in Chapter 6.

Chapter 5

Dissecting a non-Abelian quantum memory

Physical realizations of non-Abelian anyons are often highly complex, making it hard to express the states of anyons and the operations on them in terms of the underlying physical medium. However, the relative simplicity of Abelian anyon models allows their physical realizations to be well understood and easily studied. As a result of this problem, proposals for quantum memories using non-Abelian anyons are often presented only at an abstract level [39, 40]. Those using Abelian anyons, however, may be far more explicit [35, 42].

A notable exception to this rule is the non-Abelian $D(S_3)$ model, for which states and operations have been determined in terms of the underlying spin lattice [24]. We use this as an opportunity to study the physical realization of a non-Abelian quantum memory. This information will then be used to show that equivalent memories can be realized with Abelian models.

We consider quantum memories in which logical qubits are encoded in the charge anyons of the $D(S_3)$ anyon model. Two possible methods are presented for this. The method presented in Section 5.1 is such that logical information can be read out using LOCC measurements, whereas that of Section 5.2 requires non-local measurements. Since we expect the fusion channel of anyons to be a non-local degree of freedom,

we identify the latter as the 'true' non-Abelian quantum memory, and the former 'non-abelian-like'. The means to make the non-abelian-like memory as resilient to errors as the true non-Abelian memory are then investigated in Section 5.3.

It is found that, though the true non-Abelian memory explicitly requires the use of the underlying non-Abelian group structure, the non-abelian-like memory does not. This suggests the possibility of engineering the non-abelian-like memory with Abelian models. As shown in Chapter 4, the non-Abelian charges of $D(S_3)$ can be simulated using $D(Z_6)$, making this a good candidate for the realization of a non-abelian-like memory. Also, since $6 = 2 \times 3$, and hence twice an odd number, the arguments of Chapter 3 show that it is universal for quantum computation. However, we will not simply construct the memory using the quasiparticles of the enhanced $D(Z_6)$ model in Chapter 4, since these require more stabilizer information to be discarded than is necessary. A new enhanced Abelian model is therefore defined in Section 5.4 and used to define a non-Abelian like memory in Section 5.5. The resistance of this memory against local perturbations in the Hamiltonian is then presented in Section 5.6.

5.1 Non-abelian-like quantum memory with $D(S_3)$

The non-Abelian $D(S_3)$ model was introduced in Chapter 2. In Eq. 2.21 it was shown that the three charges of this model, 1, Λ and Φ, satisfy the fusion rules,

$$\Lambda \times \Lambda = 1, \;\; \Lambda \times \Phi = \Phi, \;\; \Phi \times \Phi = 1 + \Lambda + \Phi.$$

The last implies that the Φ charges have three possible fusion channels; a pair may fuse to the trivial charge 1, a Λ or a Φ. This may be used to define a quantum memory.

Definition of logical states

Logical states are defined by the action of the creation operators W^{Φ} and W^{Λ} on vertices initially in the vacuum state $|\,gs\rangle$. For the definitions of these, see Chapter 2.

Consider four neighbouring vertices, as shown in Fig. 5.1. Applying W^{Φ} to spins 1 and 4 creates two pairs of Φ charges from the vacuum, one on vertices v_1 and v_2 and the other on v_3 and v_4. Since these pairs are created from the vacuum, they both carry the vacuum fusion channel. This state is identified with the logical qubit state $|\,0_L\rangle$.

Applying W_i^{Λ} to spin 2 creates a pair of Λ charges. One of these will fuse with the Φ on v_2 and the other with the Φ on v_3. After the fusion, the two Φ pairs carry the Λ fusion channel. This state is identified with the logical qubit state $|\,1_L\rangle$. The same is achieved if the W_i^{Λ} is applied to 4. The encoded states for the logical qubit may then be explicitly written as,

$$\begin{aligned} |\,0_L\rangle &= W_1^{\Phi} W_4^{\Phi}\,|\,\mathrm{gs}\rangle\,, \\ |\,1_L\rangle &= W_2^{\Lambda} W_1^{\Phi} W_4^{\Phi}\,|\,\mathrm{gs}\rangle\,. \end{aligned} \tag{5.1}$$

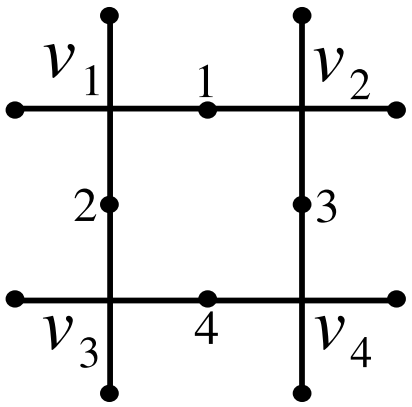

Figure 5.1: Four vertices use to store a logical qubit.

Rather than keeping the Φ charges on neighbouring vertices, it is possible to move them apart. All operations acting on a single spin, i, above must then act on a corresponding chain of spins, C_i, lying on a path connecting the anyons. The operations $W^{\Phi}_{C_i}$ and $W^{\Lambda}_{C_i}$ then take the form,

$$\begin{aligned} W^{\Lambda}_{C_i} &= \prod_{j\in C_i} W^{\Lambda}_j, \\ W^{\Phi}_{C_i} &= \sum_{g_n\times\ldots\times g_1=c^k} (\omega^k+\omega^{-k})\,|\,g_1,...,g_n\rangle\,\langle g_1,...,g_n\,|\,, \end{aligned} \tag{5.2}$$

where $g_1,...,g_n$ are the states of the spins within the chain C_i and $\omega = e^{i2\pi/3}$. The logical states take the same form as Eq.(5.1) except that operations acting on spins i will instead act on the chains C_i.

Logical Pauli operations

The logical X operation corresponds to any process that creates two Λ charges and fuses both with a Φ from each pair, such as $X = W^{\Lambda}_{[C_2]}$. As such this operation is protected against errors as the pairs are moved apart, as it becomes more difficult for Λ's to move or tunnel from one pair to another. Since W^{Λ}_i is an observable, measurement in the X basis may be achieved by measuring the eigenvalue of W^{Λ}_i on each spin in a chain connecting a Φ from each pair and calculating the parity.

The logical Z operation corresponds to vertex operators acting on both Φ charges of either pair,

$$Z = T_t(v_1)T_t(v_2) \text{ or } T_t(v_3)T_t(v_4). \tag{5.3}$$

Such an operation corresponds to the flux anyons of plaquettes braiding around v_1 and v_2, or v_3 and v_4. This could be either a single braiding around both or two independent braidings around each.

Since the logical qubit is encoded in the fusion channel, measurement in the Z basis is achieved through fusion of the charge pairs. This is achieved by moving the two Φ charges of each pair onto the same vertex and measuring the result. Fusing the Φ charges on v_1 and v_2 and obtaining the vacuum or a Λ implies a logical qubit

state of $|0_L\rangle$ or $|1_L\rangle$, respectively.

Logical measurements with LOCC

As well as measurement by fusion, the above relation suggests that the Z measurement can also be performed by LOCC when the Φ charges remain separated. This is because measurement of the eigenvalue of $T_t(v_1)$ and $T_t(v_2)$ (or those on v_3 and v_4) and calculation of the parity is sufficient to determine the Z basis state.

The fact that such an LOCC measurement of the Z basis exists, with only the spins around each anyon requiring measurement rather than all those in between as well, shows that this is not a true non-Abelian encoding. If it were, then only the fusion of anyons or equivalent non-local operations would be sufficient to determine the measurement outcome. Even so, we may still demonstrate that the measurement of both anyons of a pair is required rather than just one, showing that the encoding is not accessible by local operations alone. Observe that $W_i^\Lambda W_i^\Phi = W_i^\Phi$, implying,

$$W_1^\Lambda W_2^\Lambda W_2^\Phi = W_1^\Lambda W_2^\Phi. \tag{5.4}$$

Here the left-hand side creates a Φ pair on v_1 and v_2 and fuses a Λ with the Φ on v_2. The right-hand side does the same except that the Λ is fused with the Φ on v_1. The equality between these shows that the resultant state does not depend upon which Φ the Λ was fused with. It holds even when they are well-separated, showing that the encoding of information in this way is indistinguishable by operators that act only on one Φ, and hence cannot be distinguished by local operators alone. Operators that act on both Φ's in a pair are required, and so must be non-local or LOCC.

Code distance

The code distance of this encoding is the minimum number of spins that must be acted on to cause a logical error. For Z errors, this is seven spins if the two Φ charges of a pair are on neighbouring vertices, or eight spins otherwise, irrespective of the distance between the anyons. For X errors it is the minimum number of spins

in a path connecting a Φ from one pair to one from the other. The value of the code distance therefore depends on the placement of the anyons. If the Φ charges of each pair are kept on neighbouring vertices, only one spin needs to be acted on to cause a logical X, so the distance in this case is 1. If the Φ charges of each pair are well-separated it is the Z that is easiest to implement so the distance takes the value of 8.

Stabilizer code interpretation

It is illuminating to study how the above memory fits in to the formalism of stabilizer codes. The stabilizer operators here are defined by the projections onto anyon states for each vertex, as stated in Eq. 2.17. The stabilizer space corresponds to the anyonic vacuum everywhere. The particle types and positions of anyons correspond to the syndromes.

Consider an alternate projector onto the state of Λ charges,

$$P'_\Lambda(v) = \frac{1}{2}[T_e(v) - T_t(v)]. \tag{5.5}$$

The action of this on the states of anyons at a vertex v in comparison with that of the standard projector $P_\Lambda(v)$ is,

$$\begin{aligned} &P_\Lambda(v)\,|\,1_v\rangle = 0, \;\; P_\Lambda(v)\,|\,\Lambda_v\rangle = |\,\Lambda_v\rangle\,, \;\; P_\Lambda(v)\,|\,\Phi_v\rangle = 0, \\ &P'_\Lambda(v)\,|\,1_v\rangle = 0, \;\; P'_\Lambda(v)\,|\,\Lambda_v\rangle = |\,\Lambda_v\rangle\,, \;\; P'_\Lambda(v)\,|\,\Phi_v\rangle \neq 0. \end{aligned} \tag{5.6}$$

Both detect the presence of an isolated Λ on v, but whereas $P_\Lambda(v)$ does not see a Λ when a Φ is present, $P'_\Lambda(v)$ can detect a Λ hiding within, corresponding to a -1 eigenvalue of $T_t(v)$.

These projectors are equivalent except when a Φ is present, in which case the latter extracts more syndrome information than the former. The syndrome information obtained by the standard stabilizer of Eq. 2.17 is therefore equivalent to a modified stabilizer in which $P_\Lambda(v)$ is replaced by $P'_\Lambda(v)$ on all vertices except

where a Φ is present. This suppression of elements of the stabilizer on certain vertices is reminiscent of the holes considered in Chapter 3. Hence the definition of non-Abelian stabilizer codes is such that the holes in the code result whenever non-Abelian charges are created, and that these holes are not stationary but carried by the quasiparticles. Since the Hamiltonian assigns energy to any state that is not the vacuum without distinction, it does not see when a Λ hides within a Φ and when it does not. The holes therefore also hide the logical states from the Hamiltonian and keep them degenerate.

With the new projector, the LOCC measurement of Z can be seen as using $P'_\Lambda(v)$ to detect the Λ's within a Φ pair. If an even number are found it is deduced that fusing the Φ's will annihilate the Λ's and the vacuum fusion channel will result. Hence the logical qubit is in state $|\,0_L\rangle$. If only one is found, however, it is deduced that the pair is in the Λ fusion channel and hence the state $|\,1_L\rangle$.

5.2 True non-Abelian quantum memory with $D(S_3)$

To see how a stronger encoding may be constructed, let us consider the single spin operation,

$$W'^{\Phi}_i = |\,c\rangle\langle c\,| - \left|\,c^2\right\rangle\left\langle c^2\,\right|. \tag{5.7}$$

Like W^Φ_i, this creates a pair of Φ charges on the vertices either side of the spin. However, if these pairs were used for the above encoding, the Z operation would take the form,

$$Z = -T_t(v_1)T_t(v_2) \text{ or } -T_t(v_3)T_t(v_4). \tag{5.8}$$

This differs from Eq. 5.3 by a mere minus sign, which may seem unimportant. However, this is the key to preventing LOCC access to the logical information. Consider the encoding,

$$\begin{aligned} |\,0_L\rangle &= W^\Phi_1 W^\Phi_4\,|\,\mathrm{gs}\rangle\,, \\ |\,1_L\rangle &= W^\Lambda_2 W'^\Phi_1 W'^\Phi_4\,|\,\mathrm{gs}\rangle\,. \end{aligned} \tag{5.9}$$

This uses Φ pairs created by W_i^{Φ} to store $|\,0_L\rangle$ and Φ pairs created by W'^{Φ}_i to store $|\,1_L\rangle$. These are both states on which $T_t(v_1)T_t(v_2)$ and $T_t(v_3)T_t(v_4)$ act trivially, so neither one now performs the logical Z. Instead this requires a non-local operation, such as bringing the two Φ charges of a pair together, fusing them on a vertex v_i, applying $T_t(v_i)$ to the fusion outcome, recreating the Φ pair and returning them to their original positions. In terms of the braiding of flux anyons, this means that the logical Z can only be realized by a braiding around both v_1 and v_2, or v_3 and v_4, together. Unlike in the previous encoding, two independent braidings are insufficient.

With this new encoding, the LOCC measurement of the Z basis no longer works. The relative minus sign of the state in Eq. 5.7 tricks the $P'_{\Lambda}(v)$ projectors into thinking one more Λ is present in the pair than there is, and so both the logical states of Eq. 5.9 always appear to contain an even number of Λ's. The only way to measure in the Z basis is then to fuse the Φ charges. This is the true non-Abelian encoding. Note that the huge operational difference between this encoding and that of Eq. (5.1) comes directly from the non-Abelian group multiplication underlying the model. It is only because of this that the relative minus sign in Eq. (5.7) has such an effect. Abelian group multiplication cannot provide tricks to fool the $T_t(v)$ observables in such a way.

The stronger encoding increases the complexity of the logical X operation. The fusion of a Φ with a Λ by simply placing them on the same vertex is no longer enough. The unitary operation,

$$U(v) = \frac{1}{3}T_e(v) - \frac{2}{3}[\omega\, T_c(v) + \omega^2\, T_{c^2}(v)], \tag{5.10}$$

must be applied to any vertex on which a fusion takes place to rotate from W_i^{Φ} type Φ pairs to W'^{Φ}_i type, or vice-versa.

Previously the logical X acting on as many spins as was required to form a path between the quasiparticles. Hence, when the quasiparticles were neighbouring, only one spin was required. This allowed the gates of of Section 3.4 to be implemented

on a minimum of one lattice spin per logical qubit. Now, however, there is an extra overhead in order to implement $U(v)$, meaning a minimum of four spins are required for the logical X, and the gates of of Section 3.4. Such non-topological operations are therefore much more impractical to implement on the true non-Abelian encoding than the non-abelian-like encoding.

The new encoding also has a significant effect on the code distance, since it means that the number of spins that must be acted on to perform a Z error depends on the separation of the Φ. If we use l to denote the minimum number of spins on a path between a Φ charge of one pair with that of the other, the code distance may be expressed as $O(l)$, and so may be made arbitrarily large.

5.3 Closing the gap between the memories

The two encodings presented above are very similar, with both storing a logical qubit in the fusion channel of four Φ charges. However, the maximum code distance for the former is fixed at 8, whereas for the latter it can take an arbitrarily high value. The reason for this difference is that, for the former, the logical Z may be achieved by a product of two operations, each performed on the spins surrounding one anyon of each pair. However, for the latter, it requires an operation that acts not only on the spins surrounding the anyons, but those connecting them. We now consider the means to improve the non-abelian-like memory, and give it a comparable code distance to the true non-Abelian memory.

Definition of logical states

In order to increase the distance of the non-abelian-like encoding, each qubit could be stored on $2N$ pairs of Φ charges, rather than just 2. For example, consider the use of 4 pairs of Φ charges, on the vertices depicted in Fig. 5.2. The logical states,

now using the enumeration of Fig. 5.2 are,

$$\begin{aligned} |\,0_L\rangle &= \frac{1}{4}(1+W_2^\Lambda)(1+W_9^\Lambda)W_1^\Phi W_3^\Phi W_8^\Phi W_{10}^\Phi\,|\,\mathrm{gs}\rangle\,, \\ |\,1_L\rangle &= W_4^\Lambda(1+W_2^\Lambda)(1+W_9^\Lambda)W_1^\Phi W_3^\Phi W_8^\Phi W_{10}^\Phi\,|\,\mathrm{gs}\rangle\,. \end{aligned} \tag{5.11}$$

Again, moving the anyons away from each other means that operations here on single spins i are instead performed upon a chain C_i.

The pair of Φ charges on v_1 and v_2 in the previous encoding is replaced here by a row of four, on $v_1,\ldots,v_4$. A projection, $(1+W_2^\Lambda)/2$ is made on the spin connecting these pairs. This ensures that neither has a well defined fusion channel and the whole row must be fused for a definite answer. The $|\,0_L\rangle$ state is identified with the fusion of all four Φ's to the vacuum, and the $|\,1_L\rangle$ with their fusion to a Λ. The same is true for the four Φ's on the bottom row. The logical Z operation then takes the form,

$$Z = T_t(v_1)T_t(v_2)T_t(v_3)T_t(v_4) \text{ or } T_t(v_5)T_t(v_6)T_t(v_7)T_t(v_8). \tag{5.12}$$

When the anyons are on neighbouring vertices, this acts on a minimum of thirteen spins. Otherwise a minimum of sixteen is required. When $2N$ pairs are used, these numbers become $3N+1$ and $4N$, respectively. The X operation is implemented by fusing a Λ with a Φ from each row and so, as before, requires action on an increasing number of spins as the rows are separated by distance l.

Code distance

In the new encoding, the number of spins that must be acting on to implement a logical Z is $O(N)$, and that to implement a Z is $O(l)$. Hence by increasing the number of pairs in each row and the distance between the rows, the code distance may be made arbitrarily high. Long rows of Φ charges in the non-abelian-like encoding therefore have the similar error protection properties to a well separated Φ pair in the true non-Abelian encoding.

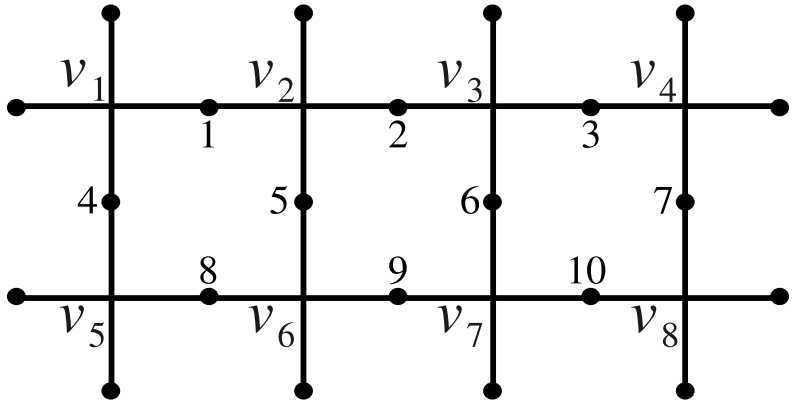

Figure 5.2: Eight vertices are shown, each of which holds a Φ in the extended encoding.

Detection and correction of errors

In some cases, partially performed logical operations leave a trace in the form of anyons. Detection of these can be used to deduce the error and correct it. For example, consider the creation of a Λ pair, where one Λ fuses with a Φ and the other remains free. Any detection of the remaining Λ shows that a logical X has partially occurred. By fusing it with the nearest Φ, one corrects the error with a good probability. Similarly, logical Z errors can be implemented by the braiding of flux anyons around the Φ charges. The presence of such fluxes may signal that partial braidings have been performed. Fusing them by the shortest path should undo such errors with good probability.

For the non-abelian-like encoding, however, some partially performed logical operations leave no anyonic trace. These include partial Z errors, which correspond to applications of single T_t operations. To see the effect of these consider the application of $T_t(v_1)$ on vertex v_1, or any other holding a Φ. If a logical X is implemented by fusing a Λ at v_1 then it will anticommute with the T_t. Measuring X along a chain of spins from v_1 will therefore give the wrong result. To deal with this, majority voting could be employed. The X could be measured in every possible way and

the most frequent outcome taken as the correct one. The probability of the wrong outcome will then be exponentially suppressed by N.

For an alternative to this, consider the encoding with four pairs as in Fig. 5.2. A projection $(1+W_i^\Lambda)/2$ is made on spins 1, 2, 3, 8 9 and 10. This places the state of all these spins, or the corresponding chains when separated, in the $+1$ eigenspace of W_i^Λ. Since W_i^Λ anticommutes with T_t, the application of this on any vertex will result in the state of the spins either side moving to the -1 eigenspace of W_i^Λ. Hence by measuring the W_i^Λ observables on all such spins it is possible to determine when and where T_t operations have occurred with good probability, and hence correct them. This can also be used to energetically suppress such errors, as we will explore in Section 5.6

5.4 An enhanced Abelian model of $D(Z_6)$

The Abelian $D(Z_6)$ model can be used to realize quasiparticles with which a non-abelian-like memory may be constructed. The enhanced Abelian model used for this is defined as follows,

$$\begin{aligned} M_1 &= \{1\},\ M_\phi = \{e^1, e^4\},\ M_{\overline{\phi}} = \{e^2, e^5\},\ M_\lambda = \{e^3\}, \\ M_\chi &= \{e^1, e^4\},\ M_{\overline{\chi}} = \{e^2, e^5\},\ M_\mu = \{e^3\}. \end{aligned} \tag{5.13}$$

This leads to the fusion rules,

$$\begin{aligned} \phi \times \overline{\phi} &= 1 + \lambda, \quad \phi \times \lambda = \phi, \quad \overline{\phi} \times \lambda = \overline{\phi}, \\ \overline{\phi} \times \overline{\phi} &= \phi, \quad \phi \times \phi = \overline{\phi}, \quad \lambda \times \lambda = 1. \end{aligned} \tag{5.14}$$

Since the Hamiltonian of the model, as defined in Eq. 2.11, assigns the same energy to each of the anyons, arbitrary states of the quasiparticles will also be eigenstates of the Hamiltonian.

States with $(\phi, \overline{\phi})$ or λ pairs on vertices connected by a single edge, i, can be

created by acting on the ground state with the operators:

$$W_i^{\phi} = \frac{1}{2}\sigma_i^z \left[1 + (\sigma_i^z)^3\right], \; W_i^{\lambda} = (\sigma_i^z)^3, \tag{5.15}$$

respectively. The projection $(1+(\sigma_i^z)^3)/2$ present in W_i^{ϕ} may be performed deterministically by measuring the observable $(\sigma_i^z)^3$ and applying $\big(A(v)\big)^3$ to a neighbouring vertex if the -1 eigenvalue is obtained.

Quasiparticles χ, $\overline{\chi}$ and μ on plaquettes can be defined equivalently to ϕ, $\overline{\phi}$ and λ, respectively. The corresponding creation operators W_i^{χ} and W_i^{μ} are obtained from Eq. 5.15 using the substitution $\sigma_i^z \to \sigma_i^x$. The braiding of the quasiparticles can be determined from the constituent e_g and m_g anyons. For example, a μ around a λ gives the statistical phase $e^{i\pi}$ due to their identification with m_3 and e_3, respectively.

5.5 Non-abelian-like quantum memory with $D(Z_6)$

As for the $D(S_3)$ charges, the non-abelian-like memory can be defined using two rows of quasiparticles, consisting of $2N$ pairs. For example, the logical states for four pairs are,

$$\begin{aligned} |\,0_L\rangle &= \frac{1}{4}(1+W_2^{\lambda})(1+W_9^{\lambda})W_1^{\phi}W_3^{\phi}W_8^{\phi}W_{10}^{\phi}\,|\,\mathrm{gs}\rangle\,, \\ |\,1_L\rangle &= W_4^{\lambda}(1+W_2^{\lambda})(1+W_9^{\lambda})W_1^{\Phi}W_3^{\phi}W_8^{\phi}W_{10}^{\phi}\,|\,\mathrm{gs}\rangle\,. \end{aligned} \tag{5.16}$$

The enumeration of the spins and vertices is as in Fig. 5.2. The logical states are defined in exact correspondence with those in Eq. 5.11, the only difference being the distinction between ϕ and $\overline{\phi}$ that exists here. Even numbered vertices hold ϕ quasiparticles in this encoding, and odd numbered ones hold $\overline{\phi}$ quasiparticles. The fusion channels of χ's and $\overline{\chi}$'s may similarly be used to encode p-type qubits on corresponding plaquettes $p_1, \ldots, p_8$.

When the rows are neighbouring, as in Fig. 5.2, the logical qubit operations are

given by,

$$\begin{aligned} X &= W_i^{\lambda} \;\; i \in \{4,5,6,7\}, \\ Z &= A^3(v_1)A^3(v_2)A^3(v_3)A^3(v_4) \text{ or } A^3(v_5)A^3(v_6)A^3(v_7)A^3(v_8). \end{aligned} \tag{5.17}$$

Moving the rows apart means that the X operations become products of W_i^{λ} on any chain of spins connecting the two rows.

Note that λ and μ together form a submodel equivalent in braiding and fusion to the e and m anyons of the $D(Z_2)$ model. Since each row of the $(\phi, \overline{\phi})$ pairs belongs to the vacuum or λ fusion channel, and each row of $(\chi, \overline{\chi})$ pairs corresponds to the vacuum or a μ, braiding of these rows is equivalent to the braiding of vertex and plaquette holes in $D(Z_2)$. Hence the methods used for quantum computation in Chapter 3 may be applied here, while the non-abelian-like quantum memory provides fault-tolerance and the potential to move the rows of quasiparticles with decoherence using adiabatic techniques.

5.6 Fault-tolerance

We consider errors that do not excite the system, requiring a temperature low enough for topological order to be stable [16, 58]. Perturbations in the Hamiltonian of the model are then the main source of errors. Though it is known that topological models are stable against these [59], their specific effects on our encoding must be considered.

Imprecisely tuned Hamiltonians

The Hamiltonian of the model, which we denote H_{Z_6}, is defined in Eq. 2.11. This can be expressed as an equally weighted sum of the stabilizers $A(v)$ and $B(p)$. However, physical systems will likely produce perturbed Hamiltonians, lifting the degeneracy of the anyons and breaking the symmetries our scheme requires. This is a problem that not only affects realizations of $D(Z_6)$, but all quantum double models, Abelian

or non-Abelian [7, 24]. Here we present a method to enforce the symmetries in $D(Z_6)$, but the principle applies in general.

We require that the states within the computational space, are unaffected by perturbations that lift the degeneracies of the e_1 and e_4 anyon states and the e_2 and e_5 states. If this is not so, relative phases will accumulate between the superposed anyon states, causing errors in X basis measurements. For example the perturbation $\delta A^3(v_1)$ on vertex v_1 does not commute with W_1^λ. Using this to measure the logical X will therefore give the wrong result.

To see how these perturbations may be dealt with, consider the spins located on edges between each ϕ and $\overline{\phi}$ in a row. According to the definition of the logical states in Eq. 5.16, the projection $(1 + W_i^\lambda)$ is applied to each of these spins. This makes the logical states eigenstates of the W_i^λ with eigenvalue $+1$. We may then consider adding the term $-BW_i^\lambda$ to the Hamiltonian on each of these spins, which will have no effect on the logical states except to reduce their energy. However, since they anticommute with any perturbations that lift the required degeneracies, the perturbations are energetically suppressed.

To study the effectiveness of these terms in suppressing the perturbation, the problem may be mapped to that of a repetition code. The logical X is the product of W_i^λ's for spins on a path connecting the two rows. For a path that starts at the vertex v_i on the top row, such a logical X may be denoted $X(v_i)$. If we consider the case for which the perturbations act only on the vertices of the top row, and not the bottom, it makes no difference at which vertex the path ends. The encoding for the X basis is therefore equivalent to a repetition code, where the N vertices v_i holding ϕ and $\overline{\phi}$ are equivalent to N qubits, with the state for each determined by the eigenvalue of the corresponding $X(v_i)$. All these should be equal, with any difference signalling the presence of errors. In this interpretation, a perturbation on a vertex v_i that lifts the required degeneracies is equivalent to a perturbation that causes a bit flip on the corresponding qubits. The W_i^λ acting on horizontal links between ϕ's and $\overline{\phi}$'s of the top row are equivalent to parity check operators that

determine whether neighbouring spins are in the same state.

In a repetition code, error correction is done by majority voting. Hence, in the limit $N \to \infty$, correction can always be achieved with unit probability when the probability of a single spin bit flip $p < 0.5$. For $p > 0.5$ the code cannot correct at all. For finite N, the probability of correction failing is exponentially suppressed in N when p is small. The majority voting can be performed without direct measurement of the spins by means of the parity check operators. Since these detect when neighbouring spins are not in the same state, they detect boundaries between chains of spins in equal state. This can be used to determine which spins are in the majority and which are in the minority.

Let us now consider the Hamiltonian which acts on the encoded information. For the degeneracy lifting perturbations, the specific case of $\delta A^3(v)$ terms is studied. Their action is trivial on all vertices which hold the vacuum and, as stated above, we consider the case that they do not act on the bottom row of ϕ's and $\overline{\phi}$'s. The total Hamiltonian is then,

$$H_{Z_6} + \sum_v \delta A^3(v) - B \sum_i W_i^\lambda, \tag{5.18}$$

where the sums are over only the vertices of the top row and the links between them, respectively. The first term in this only contributes a constant energy since there are a specific number of quasiparticles on the lattice. Since the perturbations act as bit flips and the W_i^λ as parity check operators, the Hamiltonian is equivalent to that of the quantum Ising model in a transverse field,

$$H = -B \sum_i (\sigma_i^z \sigma_{i+1}^z + g\sigma_i^x), \tag{5.19}$$

where these are spin-1/2 Pauli operators and $g = \delta/B$.

Using this equivalence, results of the well-known quantum Ising model can be applied [60]. For $g = 0$ the model has a two-fold degenerate ground state corresponding to the logical states. An energy gap of $2B$ protects these against errors.

For $0 < g < 1$ the degeneracy of the ground state space is broken, and the gap between the two lowest lying states and those above them decreases. Due to the phase transition, the gap drops significantly when $g \approx 1$, and becomes gapless at $g = 1$ in the thermodynamic limit.

The probability of a bit flip on any spin, p, is related to the probability of a parity check operator detecting an error, P, according to the relation

$$P = 2p(1-p)$$

This is related to the expectation value of the corresponding $\sigma_i^z \sigma_{i+1}^z$ according to,

$$\langle \sigma_i^z \sigma_{i+1}^z \rangle = 1 - 2P.$$

The $z-z$ correlations of the quantum Ising model may then be used to determine p as follows,

$$p = \frac{1 - \sqrt{\langle \sigma_i^z \sigma_{i+1}^z \rangle}}{2}. \tag{5.20}$$

The value of $N = 10$ was taken as a realistic example and studied numerically. Since this is a finite sized system, the values of p are not the same for all spins, and so the maximum was determined. The maximum value of p and the energy gap found are shown in Fig 5.3 and Fig. 5.4, respectively.

It is easy to see that, for the ground state of the model, the bit flip probability only reaches the uncorrectable value of $p = 1/2$ as $g \to \infty$. Hence, in the thermodynamic limit of large N, the magnetic field always ensures that the errors can be corrected, even if it is much lower than the perturbation strength. However, this will only be efficient, with errors exponentially suppressed by N, when p is sufficiently small. Hence we can interpret the $g < 1$ phase of the model as that for which the error correction properties of the model is efficient, and the $g > 1$ phase as increasingly inefficient as g increases. This is in good agreement with the fact that the former phase has strong, long range $\sigma^z \sigma^z$ interactions, whereas the latter does not.

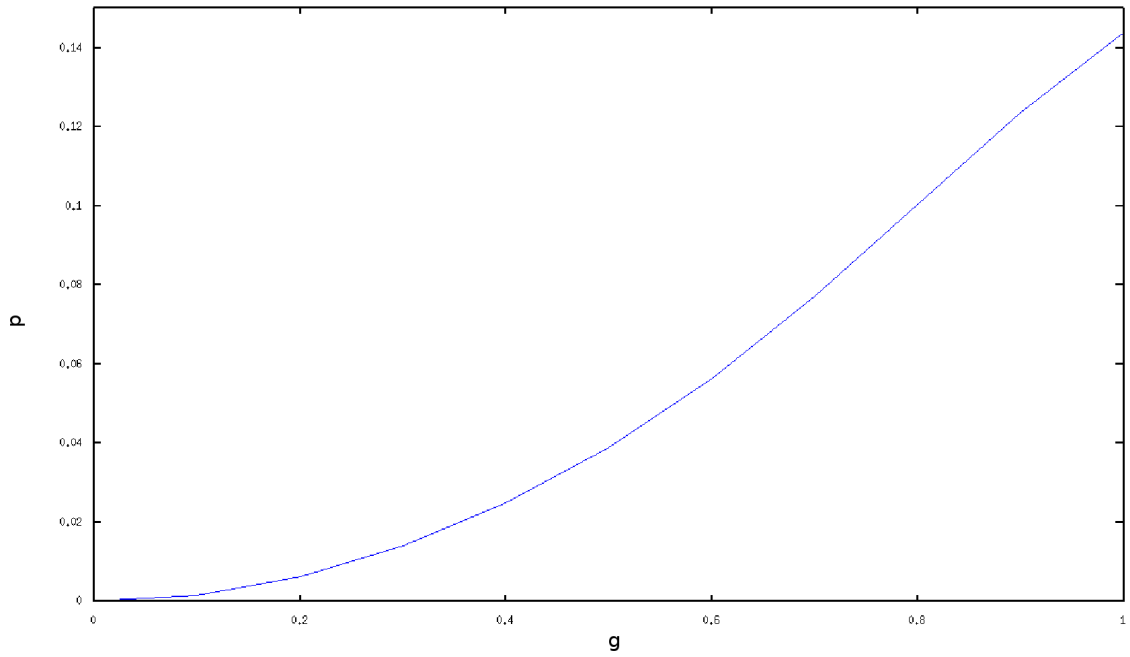

Figure 5.3: A plot of the maximum probability for a bit flip p, against the strength of the perturbation. This was found by evaluating $\sigma_1^z \sigma_2^z$ for the lowest lying eigenstate, since this gives the maximum value for p_i.

All the above arguments correspond to the highly unphysical case that perturbations act only on the $(\phi, \overline{\phi})$ pairs of the top row, and leave the bottom row unaffected. Realistically, both must be taken into account. This is done by evaluating the parity check operators provided by the W_i^λ on horizontal links separately, and evaluating the logical X between vertices in the majority on each. The probability of success will then not be so high as when a single row is effected, but the probability of error is still exponentially suppressed in N when $g < 1$.

The encoding of quantum information in square banks of quasiparticles, rather than lines, can also be considered. This would make the effect of imprecisely tuned Hamiltonians equivalent to the two-dimensional Ising model, and hence increase error suppression. However the movement of such banks may well be more complex than that of lines, and so the latter case only was considered here.

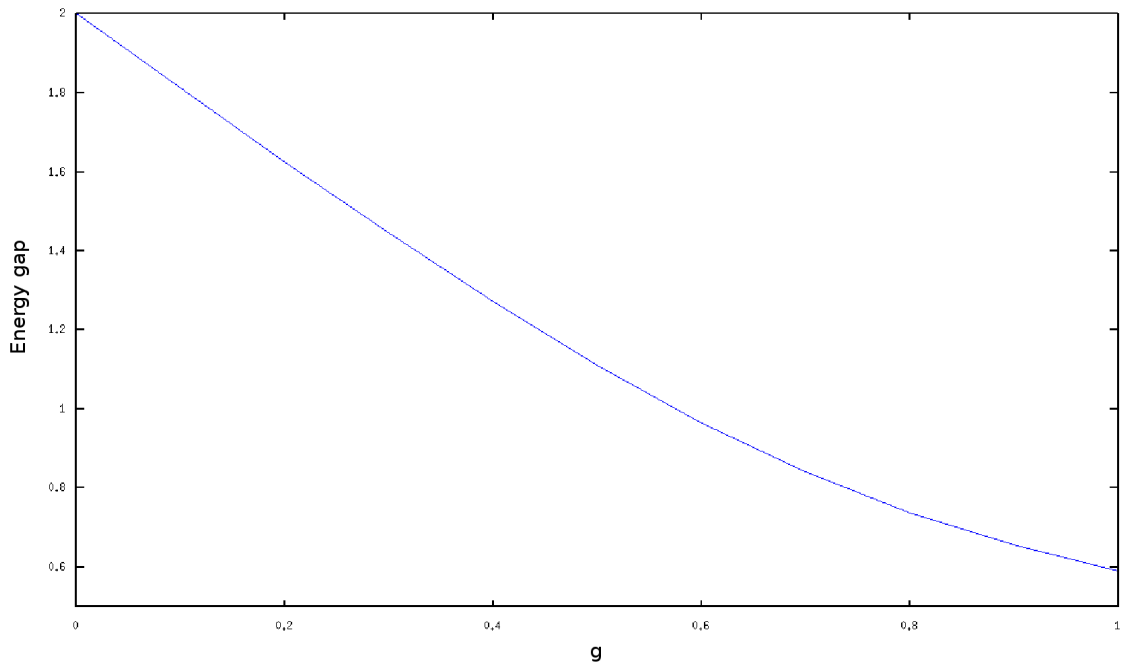

Figure 5.4: A plot of the energy gap between the two lowest lying eigenstates and those above.

Transport and annihilation of quasiparticles

The encoding we propose uses quasiparticles placed on the lattice, and hence stores information in excited states rather than the ground state space. For this reason, even single spin perturbations can have a large effect by moving the constituent anyons or causing them to fuse. To deal with such errors, the computational space must be moved into the ground state space by making some alterations to the Hamiltonian. For vertices on which a ϕ resides, the $P_{e_0}(v)$ term in the Hamiltonian should be replaced with $P_\phi(v) = P_{e_1}(v) + P_{e_4}(v)$, which similar replacements made also for the locations of $\overline{\phi}$, χ and $\overline{\chi}$ quasiparticles. The Hamiltonian will then energetically favour the presence of these quasiparticles in these locations, rather than other particle types or the vacuum.

Many body perturbations

Perturbations acting on many spins can stretch between the rows of quasiparticles or loop around them, causing the degeneracy of logical states to be affected. To determine how many spins on which these perturbations must act in order to have such an effect, the code distance must be considered. For the non-abelian-like encoding $O(l)$ spins must be acting on to cause an X basis error, where l is the minimum separation of the rows, and $O(N)$ spins must be acted on for a Z basis error.

It is reasonable to assume that nature is incapable of highly correlated errors with significant strength. Hence, by increasing l and N to be much larger than the number of spins on which perturbations act, the encoding should remain stable against them.

5.7 Conclusions

In this chapter the charge anyons of the $D(S_3)$ model were investigated in terms of the quantum memory they can provide. Two encodings were studied, a non-abelian-like memory which was found to be limited in its error correction, and a true non-Abelian memory which was fully topologically protected. The means to improve the performance of the non-abelian-like memory were then identified, giving it a resilience against errors comparable to the latter. It was then showed that this memory can be realized using Abelian anyon models, with the fault-tolerance of the encoding studied in this case.

The non-abelian-like encoding was shown to be equivalent to the holes used in Chapter 3 pinned to quasiparticles. The means by which the holes may be moved fault-tolerantly is then the same as for non-Abelian anyons, or the superpositions of Abelian anyons used in [38] and [36]. Hence as well as the operations described in Section 4.1, it is possible that local potentials and adiabatic techniques may also be used [38, 54].

The example presented in this chapter was of a memory constructed from the $D(Z_6)$ model, but this is not the only one in which such properties may be defined.

The method to construct non-abelian-like memories is applicable to all Abelian quantum double models, and would be expected to have generalizations to Abelian anyons realized by alternative means.

In studying the two encodings of the $D(S_3)$ charges it was found that, though the fusion of a Φ and Λ can be achieved by a single spin W_i^Λ operation, the true non-Abelian quantum memory also requires the many-body operation of Eq. 5.10. This result is significant in general for the use of non-Abelian models for quantum computation. It shows that realizing the operations of anyon creation, transport and fusion may not always be sufficient to achieve the full fault-tolerance expected from the anyons. Instead, the operations required for the true non-Abelian behaviour may be very specific, hard to implement and subject to errors.

As a result of this it is possible that, even when a non-Abelian model is realized, only a non-abelian-like encoding of information may be practical. This is especially true when braiding is not universal, and non-topological operations must be implemented. The increased complexity of fusion could easily make these too complex to implement for the true non-Abelian encoding, requiring the non-abelian-like memory to be used. For example, in the Josephson junction implementation of quantum double models discussed in Chapter 6, the movement and fusion of anyons requires charge pumping. This process is at the cutting edge of Josephson junction technology, yet even this would be incapable of satisfying the needs of the true quantum memory. Such a non-Abelian model will then have no advantages over Abelian models on which an equivalent non-abelian-like memory may be realized. However, the (relative) simplicity of Abelian models makes them more tractable both theoretically and experimentally. The opportunities this gives to realize such memories in the lab are further explored in Chapter 6.

Also presented here is the means by which the required Hamiltonian symmetries may be enforced. This is an important concern, since the realization of perfect Hamiltonians is not something a physical system can easily provide. Again the Josephon junctions of the next Chapter provide an example of this. The means by

which they can provide a Hamiltonian which assigns energy to anyons is well studied, but the means by which the anyons can be made degenerate has not yet been solved. However, altering the fluxes threaded through loops between the junctions can allow the method proposed here to be implemented, and so the symmetries enforced

It can be shown that our method equivalent to the transverse field Ising model, and the error correction is the same as that for a classical repetition code. Since both are well studied, their theory may be applied directly to this problem. The method we propose is general in scope, and can be applied to non-abelian-like quantum memories constructed from both Abelian and non-Abelian anyons in lattice models. The use of single spin terms in the Hamiltonian to suppress the errors is highly motivated by the practicalities of physical implementations, since such terms are usually the easiest to implement and can be made highly powerful.

The studies of this chapter also have implications for the general study of stabilizer codes. Just as the holes in the code used here were pinned to quasiparticles, quantum information in general stabilizer codes could be stored in subspaces of states with the same non-trivial syndrome, rather than simply in the stabilizer space as normal. This technique is particularly applicable to higher dimensional generalizations of stabilizer codes, such as those with spins of $d \geq 3$. The potential of the technique to improve the protection of the information and ease its manipulation, as it has done here, warrants further study.

The studies of Sections 5.1 and 5.2, dealing with a stabilizer code based upon a non-Abelian group, also highlights the ability of these codes to hide information from LOCC. It would therefore be interesting to explore their potential in terms of quantum data hiding [61], and to investigate whether quantum data hiding could be used to construct novel topological codes.

Chapter 6

Towards experimental realizations

A good deal of experimental progress has already been made in the realization of Abelian quantum double models, especially for the case of $D(Z_2)$. The results of this thesis can help build upon this progress, allowing previous experimental set-ups to demonstrate further principles of topological quantum computation, and designing simple models to realize complex anyonic behaviour. In this chapter we first present a brief overview of previous experiments in Section 6.1. Extensions to the existing single plaquette $D(Z_2)$ experiment is then proposed in Section 6.2, designed to demonstrate the principles of Chapter 3. Section 6.3 then explores the possibilities for experimental realization of the $D(Z_6)$ model, allowing the simulations of the $D(S_3)$ anyons in Chapter 4 and the non-abelian-like quantum memory of Chapter 5 to be demonstrated.

6.1 Experimental progress in quantum double models

The most explicit demonstration of the creation, braiding and fusion of anyons has been in state based approaches [27]. Rather than attempting to realize the Hamiltonian, these simply prepare the anyonic vacuum state and apply the necessary operations to manipulate the anyons. Such simulations have the same capability as

Hamiltonian based approaches to demonstrate anyonic behaviour, and to be used for topological quantum computation. However, they lose one of the main advantages: protection by the gap. To compensate for this, inherently decoherence free systems, such as photons, must be used. The challenge is then to generate the required entanglement and implement the required entangling operations with such weakly interacting systems. Thus far, state based experiments have successfully been used to demonstrate Abelian anyons and their exchange statistics. Two experiments have achieved this, both realizing the $D(Z_2)$ model with states of entangled photons [31, 32].

For realizations of the quantum doubles with a Hamiltonian, much progress has been made with Josephson junctions. The theory of how the Hamiltonians may be implemented has been developed for all Abelian models based on cyclic groups, as well as the non-Abelian $D(S_3)$ models [20]. An experiment has also been performed, realizing the $D(Z_2)$ model Hamiltonian and demonstrating the quantum memory provided by its degenerate ground state [30].

Other theoretical work towards experimental realizations is based on cold atoms. A toolkit of methods that may be used to realize anyon models with optical lattices were explored in [21]. Experiments concerning minimal instances of topological order were considered in [22]. Progress is also being made into simulations of the $D(Z_2)$ model with Rydberg atoms, in which the Hamiltonian and the effects of dissipative noise can be demonstrated [62].

6.2 Single plaquette $D(Z_2)$ experiments

The experiment of [31] deals with the $D(Z_2)$ model defined on a single plaquette without boundary conditions, as shown in Fig 6.1. This model can also be used to demonstrate the single spin measurements and hole based quantum memory of Chapter 3.

The plaquette and vertex operations for the single plaquette $D(Z_2)$ model are,

$$\begin{aligned} A(v_1) &= \sigma_1^x\sigma_4^x,\ \ A(v_2) = \sigma_1^x\sigma_2^x,\ \ A(v_3) = \sigma_2^x\sigma_3^x,\ \ A(v_4) = \sigma_3^x\sigma_4^x, \\ B(p) &= \sigma_1^z\sigma_2^z\sigma_3^z\sigma_4^z. \end{aligned} \tag{6.1}$$

The anyonic vacuum defined by these is simply the four spin GHZ state,

$$|\,gs\rangle = \frac{1}{\sqrt{2}}(|++++\rangle + |----\rangle). \tag{6.2}$$

The application of σ_i^z to any spin creates a pair of e anyons on the adjacent vertices. The application of σ_i^x creates a pair of m anyons, with one residing on the plaquette p and the other created over the edge of the model.

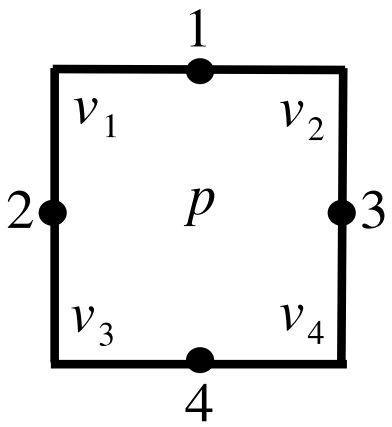

Figure 6.1: The lattice for a single plaquette $D(Z_2)$ model.

Demonstration of single spin measurements

Consider two logical qubits, a v-type qubit stored in v_1 and v_2 and a p-type qudit in p. Note that only one plaquette is required in the latter case, as the edge takes the place of the second.

Measurement of the spin 1 will result in a superposition of anyon states in v_1, v_2 and p, as in Eq. 3.15 of Chapter 3, where such measurements are used to prepare logical ancilla states. By performing state tomography of the resulting four spin state it can be verified that the measurement leads to the anyonic states expected and required by these protocols.

This experiment could easily be performed by a similar set up to the experiment in [31] with entangled photons. The measurement would leads to the loss of the corresponding photon. However, since its state is uncorrelated to the remaining three, it can easily be replaced by preparing another photon in the same state.

Demonstration of single qubit memory

The single plaquette can also be used to demonstrate a single qubit memory in the presence of the Hamiltonian. This could be done for a v-type qubit memory, but the simplest Hamiltonian is obtained for the case of the p-type memory. The single plaquette p then becomes a hole, so the corresponding plaquette operator must not feature in the Hamiltonian, which then takes the form,

$$H = -\sum_{v} A(v). \tag{6.3}$$

Since this only requires nearest neighbour $x-x$ interactions, it is an experimentally tractable Hamiltonian. It energetically suppresses the creation of e anyons which, if they braid around p, cause a logical Z error. Preparing the logical qubit in an eigenstate of X then allows the suppression of Z errors to be seen. However, X errors need only act on the single spin 2, and so are not protected against by such a small model.

Note that this experiment does not necessarily require the $D(Z_2)$ model to be defined on a square lattice, with four spins for a single plaquette. A triangular lattice could instead be used, requiring only three spins.

6.3 Experimental realizations of $D(Z_6)$

Josephson-junction realization

Josephson junctions have already been studied as a means to experimentally realize the quantum double models, especially those based on cyclic groups [20]. Proof of principle experiments for the $D(Z_2)$ model have also already been performed [30]. Here we study the realization of the $D(Z_6)$ model, both as a means to simulate the $D(S_3)$ charges as in Chapter 4 and demonstrate the quantum memory of Chapter 5.

Consider the Josephson junction element in Fig. 6.2. This consists of twelve Josephson junctions, denoted by crosses, and eight superconducting islands, denoted by dots. The dynamics of each element are described by twelve phase differences across each junction. These are labelled $\alpha_1 \dots \alpha_6$ for the junctions to the left of the element, according to the numbering of Fig. 6.2, and $\beta_1 \dots \beta_6$ for the junctions to the right.

The Josephson junctions in each element are arranged in five loops. A flux $2\pi/6$ passes through each of these, resulting in the condition,

$$\alpha_{j+1(\mathrm{mod}6)} + \beta_{j+1(\mathrm{mod}6)} - \alpha_j - \beta_j = \frac{2\pi}{6} + 2\pi n_j, \tag{6.4}$$

where the n_j are integers. A further condition comes from current conservation, which requires,

$$\sin\alpha_j = \sin\beta_j \ \ \forall j, \ \ \sum_{j=1}^{6} \sin\alpha_j = \sum_{j=1}^{6} \sin\beta_j = 0 \ \ \forall j, . \tag{6.5}$$

The Josephson energy of the system is,

$$\epsilon_J = -E_J \sum_{j=1}^{6} (\cos\alpha_j + \cos\beta_j). \tag{6.6}$$

Where E_J is the Josephson energy. Clearly, minimum energy will be obtained when

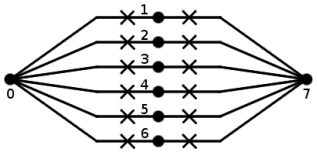

Figure 6.2: Twelve Josephson junctions arranged in five loops. This element has six degenerate ground states when a flux $2\pi/6$ is passed through each loop, and thus provides the required six-level spin.

$\cos\alpha_i > 0$ and $\cos\alpha_i > 0$ for all i. Added to the above conditions for current conservation, this implies $\sin\alpha_i = \sin\beta_i (\mathrm{mod} 2\pi)$ for all i. However, without loss of generality we can simply choose $\sin\alpha_i = \sin\beta_i$. The ground state is then obtained when the set $\{\alpha_1, \ldots, \alpha_6\}$ and coincides with the set $\{-\frac{5}{6}\frac{\pi}{2} + j\frac{\pi}{6} \mid 0 \leq i \leq 5\}$. There are six ways to map the former onto the latter, related to each other by cyclic permutations. These correspond to the six degenerate ground states of each element. All six of these choices satisfy the condition of Eq. 6.4. For all but one case, this is done with $n_i = 0$. In the exception, $n_j = 1$. This corresponds to a vortex between the jth and $j+1$th branches of the element. The value of j is different for each of the ground states, and so can be used to label the basis states of the effective six-level spin.

Constructing a lattice of such elements, as in Fig. 6.3, introduces further loops involving junctions from each element around a plaquette. If no flux is passed through each plaquette, the sum of phase differences around each will be zero. This corresponds to the state of no flux anyons in each plaquette. Only the charge anyons of vertices need therefore be considered. The Hamiltonian here originates from fluctuations in the phase variables on each island due to charging energies. Despite generating single island terms, the condition in Eq. 6.4 allows the fluctuations to only occur on all islands around a vertex at once. This leads to the following effective Hamiltonian for the six-level spins on each link.

$$H = -r \sum_v \big(A(v) + A^\dagger(v)\big). \tag{6.7}$$

Here the coupling constant r is determined by the tunnelling between degenerate ground states. By means of a semi-classical approximation [20], this may be expressed in terms of the action of the tunnelling process, S_0, as,

$$r \approx E_J^{3/4} E_C^{1/4} \exp(-S_0), \tag{6.8}$$

where E_J and E_C are the Josephson and charging energies, respectively.

During the tunnelling process, all α_i and β_i are changed. For all phases where $i \neq j$, this change is by the same amount. The exception is for $\alpha_j = \beta_j = \frac{5}{6}\frac{\pi}{2}$, the phases on the junctions below the vortex. For the ground state to change, the vortex must move between loops through a Josephson junction. This breaks the symmetry in the tunnelling process while the vortex moves, requiring an additional phase difference of 2π to be added to either α_i or β_i. We choose this to occur to β_i without loss of generality. The quantity $(\alpha_i - \beta_i)/2 = 0$ therefore stays constant during tunnelling for $i \neq j$, but changes from 0 to π for j. The tunnelling process can be approximated by formulating it entirely in terms of the change in this quantity, which we denote v. The effective energy landscape for this transition, as determined from the Josephson energy, is the following double well potential,

$$U \approx \frac{4.213 E_J}{\pi^4}(v^2 - \pi v)^2, \tag{6.9}$$

The kinetic term is,

$$K = \frac{\hbar^2}{8E_C}(\frac{dv}{dt})^2. \tag{6.10}$$

Using these, the action can be calculated using the instanton method [63], which yields,

$$S_0 \approx 0.380\hbar\sqrt{\frac{E_J}{E_C}}. \tag{6.11}$$

Single qudit σ_i^z operations, required to create anyons, can be applied by pumping charge between the vertices [64]. When using these Josephson junctions to realize the non-Abelian like quantum memories of the last chapter, it must be noted that

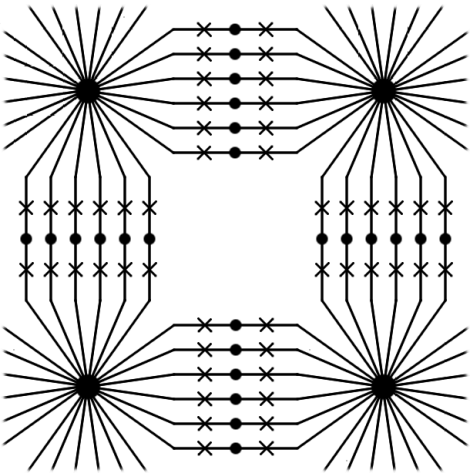

Figure 6.3: (a) Twelve Josephson junctions arranged in five loops. This element has six degenerate ground states when a flux $2\pi/6$ is passed through each loop, and thus provides the required six-level spin. (b) A plaquette of the $D(Z_6)$ model realized with Josephson junction elements.

the Hamiltonian of Eq. 6.7 is not ideal, since it does not assign equal energy to each anyon type. This therefore gives an opportunity to demonstrate the enforcement of the degeneracies by the $-BW_i^\lambda$ terms. These can be simply implemented by passing a flux of $2\pi/3$ through the elements on the links for which this term is to be applied, rather than $2\pi/6$.

Since the simulation of the $D(S_3)$ charges does not require coherence between the anyon states, the lack of the degeneracy is not important and need not be addressed. Demonstrating the creation of the quasiparticles, their transport and fusion would be an important step forward in the physical realization of non-Abelian anyons.

One-dimensional $D(Z_6)$ model

Though the exchange statistics of quasiparticles cannot be demonstrated in one-dimensional systems, their fusion can. A one-dimensional realization of $D(Z_6)$ would therefore be capable of demonstrating the fusion rules of the $D(S_3)$ charges. Also, since the non-abelian-like quantum memory of Chapter 5 does not involve braiding, its principles may be demonstrated in the one-dimensional model.

For the definition of the model, consider the line of six-level spins in Fig. 6.4.

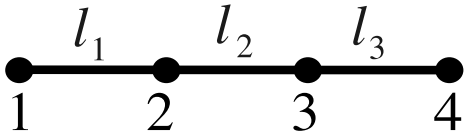

Figure 6.4: Four spins along a line, which can be used to realize the anyons of $D(Z_6)$ on the links.

Operators corresponding to vertex operators in two-dimensions are defined on neighbouring spins in one-dimension,

$$A(l_i) = (\sigma_i^x)^\dagger(\sigma_{i+1}^x). \tag{6.12}$$

The e^g anyons live on the links l_i between the spins. The application of $(\sigma_i^x)^g$ creates an e^g anyon on the link l_{i-1} and an e^{-g} on the l_i.

Ideally, the Hamiltonian of the model would be,

$$H = -\sum_i \sum_{h \in Z_6} A^h(l_i). \tag{6.13}$$

This has the anyonic vacuum as its ground state, and assigns equal energy to all anyon types. However, since the simulation does not require coherent states of the quasiparticles, Hamiltonians without the degeneracy of the anyon states could be used if experimentally simpler to realize.

Clearly this is a simple model in comparison with others used to realize quasiparticles with the properties of interest in topological quantum computation, since it requires only simple two body interactions. It therefore marks a realistic starting point for experimental demonstrations of non-Abelian anyons.

6.4 Conclusions

The theoretical arguments of all previous chapters, as in all of physics, are only significant if they can be demonstrated with real physical systems. However, since a full realization of anyon models requires control over a large number of particles with highly complex interactions, only proofs of the principles proposed in this thesis are realistic with current technology.

In this chapter the minimal resources required for proof of principle experiments are explored. A single plaquette $D(Z_2)$ model is shown to have the potential to demonstrate the action of the single spin measurements useful for the proposals of Chapter 3. This experiment is a straightforward extension to ones that have already been performed [31], and so could be implemented in the near future. The single plaquette also allows the possibility of a quantum memory using holes in $D(Z_2)$ to be demonstrated by physical systems capable of nearest neighbour $x-x$ interactions on three or more spins.

It was also found that non-Abelian behaviour could be experimentally demonstrated using six level spins. In order for a full realization of the required $D(Z_6)$ model in two-dimensions, a Josepshon junction based scheme was proposed building on existing theoretical and experimental work [20, 30]. This could be used both for a simulation of the $D(S_3)$ charge submodel and non-abelian-like quantum memories. A simpler set-up in one dimension was also proposed for proof of principle demonstrations of non-Abelian anyonic behaviour without the need for a full two-dimensional realization.

These experiments would allow the realization of anyonic behaviour in the laboratory to progress greatly over the next few years. Rather than just the scant evidence of non-Abelian behaviour available presently [33], explicit and direct observations could be made. This would form a major stepping stone to future breakthroughs in the implementation of topological quantum computation.

Chapter 7

Conclusions

7.1 Main results

The aim of this thesis has been to prove that Abelian anyon models are capable of much of the same richness and complexity of behaviour as their non-Abelian counterparts. This was done from the perspective of quantum information, where the similarities and differences between Abelian and non-Abelian models could be studied from an operational point of view.

Firstly, Chapter 3 considered the use of Abelian anyons for quantum computation. Following on from previous proposals based on the $D(Z_2)$ model [35, 36, 38, 42], this study looked in general at all Abelian quantum double models. The dependence of computational power on the kind of non-topological operations allowed and the properties of the group underlying the model could then be seen. It was found that the $D(Z_2)$ model is by no means unique in allowing universal quantum computation. The means to achieve this with simple non-topological operations was found and proven for a wide class of models. From the perspective of implementing universal quantum computation, therefore, Abelian anyons are as powerful as the non-Abelian models whose braiding is not sufficient for universality.

Chapter 4 then considered a more limited task, the ability of Abelian models to simulate non-Abelian anyons. This process again required the addition of operations

beyond those normally used in Abelian models, in this case those that allowed the creation and transport anyonic superpositions, as well as framing operations to provide chirality when required. Two examples of non-Abelian anyon simulation were provided, one of the $D(S_3)$ charge submodel and the other of the Ising anyon model. The former consists of anyons whose braiding suffices only to represent the permutation of the anyons, implementing no further operations on the fusion space. This simplicity leads to a straightforward simulation, in which merely creating superpositions, or even mixtures, of the Abelian $D(Z_6)$ charge anyons leads to quasiparticles that are indistinguishable from the $D(S_3)$ charge anyons. The simulation of the Ising model, however, realizes more complex braiding behaviour, namely non-trivial action on the fusion space and chirality. However it is shown that the non-chiral and Abelian $D(Z_2)$ model can demonstrate this behaviour when supplemented with the correct methods. Both of these simulations have their limitations, and cannot reproduce the behaviour of the anyon model in all instances, but they serve as a useful lesson of how non-Abelian behaviour may be simply realized on spin lattices, and allows simplified experimental demonstrations to be designed.

In the first few sections of Chapter 5 the non-Abelian $D(S_3)$ model was studied, with the quantum memory of the charge anyons studied in detail. Since this model is based on the simplest non-Abelian group, it is the most tractable of all non-Abelian quantum double models. It is also the most well understood of all non-Abelian models at the level of its underlying physical medium, in this case a spin lattice. It was found that the same fusion outcomes of the same anyons can be used to define two quantum memories with large operational differences. One, termed the true non-Abelian memory, has a code distance that scales with anyon separation and logical states that can only be distinguished non-locally. The other, called non-abelian-like, has instead a constant code distance and is susceptible to LOCC measurements. This is an important result concerning non-Abelian encoding of quantum information, especially in non-universal non-Abelian models. It shows that one cannot simply fuse anyons in an arbitrary manner in order to be confident

that the encoding is non-local and fault-tolerant, but extra steps may need to be taken. The operations that must be implemented in in order to ensure proper fusion and hence fault-tolerance may then make the additional non-topological operations for non-universal models too complex to be practical. The way in which the non-abelian-like encoding may be extended in order to compare favourably with the true non-Abelian encoding was then determined. These methods can then be adapted in future experimental realizations of non-Abelian anyons, both with $D(S_3)$ and otherwise, to ensure fault-tolerance.

While these results point out potential weaknesses in the memories of non-universal non-Abelian anyons, they also hint at the strengths that may be achieved by Abelian anyons. Though the true non-Abelian memory requires a non-Abelian group structure underlying the model, the non-abelian-like memory does not, and so may be realized using Abelian models. This potential was explored in the final sections of Chapter 5, in which the $D(Z_6)$ model was used to implement the extended non-abelian-like memory. This demonstrates that Abelian models not only have the same power in manipulating quantum information as their non-universal non-Abelian counterparts, but the same power in the fault-tolerant storage of that information.

With these manifestations of non-Abelian behaviour in Abelian models, the experimental advantage of the latter is then explored in Chapter 6. Experiments are proposed using current cutting edge techniques using Abelian anyons and other models that could realistically be implemented in the lab. These demonstrate the theory developed in the thesis, allowing the principles behind the computation schemes of Chapter 3 to be physically realized, as well as the quasiparticles of Chapters 4 and 5 which simulate non-Abelian anyons and realize equivalent quantum memories.

7.2 Further results

While achieving the aims of the thesis, other notable results where uncovered. In the simulations of Chapter 4, the Abelian models both had the same total quantum

dimensions as the non-Abelian models they were used to simulate. This suggests a fundamental connection between seemingly unrelated models which share only the value of this quantity. There is no reason in the abstract theory of anyons as to why this should be so, but perhaps the answer lies instead in the field of entanglement theory. It is known that the states of a physical medium required to realize anyon models must not only be highly entangled, but entangled in a certain way. This topological entanglement is measured by a quantity known as the topological entropy [14, 15], whose value is related only to the total quantum dimension of the model realized. The simulatability of one model with a certain value of the total quantum dimension by another of equal value suggests that equally topologically entangled states are equivalent up to the quasilocal operations employed to implement the simulation. However, it would not be expected that a realization of the Ising model could simulate $D(Z_2)$, since the single σ anyon of the Ising model would need to be split to form the e and m of $D(Z_2)$. Also, no way is known in which the $D(S_3)$ charges can simulate those of $D(Z_6)$. The equivalences between the states would therefore appear to be one way. These results therefore give hints as to the structure of the topological class of entanglement, though much further study would be required before the definite nature of the relationships are known.

The studies of Chapter 5 is applicable to the generalization stabilizer codes to higher dimensional spins. The true non-Abelian quantum memory shows the dramatic effect that stabilizers with a non-Abelian group structure can have in fault-tolerantly storing information. These chapters also demonstrate that information storage need not be limited to the stabilizer space in the anyonic case, for which holes in the code are required to allow additional storage. Instead it was found that quasiparticles can effectively carry holes in their internal states. Since these holes are pinned to excitations, they are well suited to being moved by local potentials or adiabatic techniques. This is in contrast with bare holes that are not pinned to quasiparticles, which are prone to decohere when moved in such a manner. Once these holes are used for encoding, it is found that certain symmetries of the Hamilto-

nian must be enforced in order to ensure fault-tolerance. More elements must then be added to the stabilizer in order to control these. Hence we see that stabilizer codes for higher dimensional spins have a richness of behaviour that goes far beyond their spin-1/2 counterparts, and deserve to be studied both within and beyond the anyonic formalism.

7.3 Final remarks

Finally we conclude by again underlining the potential of Abelian anyons for the task of quantum computation. Though universal non-Abelian models are admittedly the holy grail of topological quantum computation, and rightly so, this thesis has shown that Abelian models are just as useful as non-universal non-Abelian models. For, despite the fact that the latter have the true non-Abelian encoding at their disposal, this can be impractical to use along with the non-topological operations required for universality. The non-abelian-like memory may then need to be used instead, preventing non-Abelian anyons, or at least those realized on spin lattice models, from having major advantages over their Abelian counterparts. Abelian models, on the other hand, will always have the advantage of experimental simplicity. Hence Abelian models are a computationally powerful, fault-tolerant and experimentally realistic prospect for quantum computation.

Bibliography

[1] J. R. Wootton and J. K. Pachos, Proceedings of 6th Workshop on Quantum Physics and Logic, arXiv:0904.4373 (2009).

[2] J. R. Wootton, V. Lahtinen, Z. Wang and J. K. Pachos, Phys. Rev. B **78**, 161102(R) (2008).

[3] J. R. Wootton, V. Lahtinen, and J. K. Pachos, LNCS 5906, 56-65 (2009).

[4] J. R. Wootton, V. Lahtinen, B. Doucot and J. K. Pachos, arXiv:0908.0708 (2009).

[5] F. Wilczek, Phys. Rev. Lett. **49**, 957 (1982).

[6] E. Witten, Commun. Math. Phys. **121**, 351 (1989).

[7] A. Kitaev, Ann. Phys. **303**, 2 (2003).

[8] M. H. Freedman, A. Y. Kitaev, M. J. Larsen and Z. Wang, Bull. Amer. Math. Soc. **40**, 31 (2004).

[9] V. Kalmeyer and R. B. Laughlin, Phys. Rev. Lett. **59**, 2095 (1987).

[10] X.-G. Wen, F. Wilczek, and A. Zee, Phys. Rev. B **39**, 11413 (1989).

[11] G. Moore and N. Read, Nucl. Phys. B **360**, 362 (1991).

[12] M. Levin and X.-G. Wen, Phys. Rev. B **71**, 045110 (2005).

[13] P. Fendley, Ann. Phys. **323**, 3113 (2008).

[14] A. Kitaev and J. Preskill, Phys. Rev. Lett. **96** 110404 (2006).

[15] M. Levin and X.-G. Wen, Phys. Rev. Lett. **96**, 110405 (2006).

[16] S. Iblisdir, D. Perez-Garcia, M. Aguado and J. Pachos, Phys. Rev. B **79**, 134303 (2009).

[17] P. Bonderson, Phys. Rev. Lett. **103**, 110403 (2009).

[18] H. Yao and X.-L. Qi, arxiv:1001.1165 (2010).

[19] E. Rowell, R. Stong and Z. Wang, Comm. Math. Phys. **292**, 343 (2009).

[20] B. Doucot, L. B. Ioffe and J. Vidal, Phys. Rev. B **69**, 214501 (2004).

[21] A. Micheli, G. K. Brennen and P. Zoller, Nat. Phys. **2**, 341 - 347 (2006).

[22] B. Paredes and I. Bloch, Phys. Rev. A, **77**, 023603 (2008).

[23] M. Aguado, G. K. Brennen, F. Verstraete and J. I. Cirac, Phys. Rev. Lett. **101**, 260501 (2008).

[24] M. Aguado, G. K. Brennen, F. Verstraete and J. I. Cirac, Rev. Lett. **101**, 260501 (2008); G. K. Brennen, M. Aguado, and J. I. Cirac, New J. Phys. **11**, 053009 (2009).

[25] A. Kitaev, AIP Conf. Proc. **1134**, 22 (2009).

[26] O. Buerschaper and M. Aguado, Phys. Rev. B **80** 155136 (2009).

[27] D. W. Berry, M. Aguado, A. Gilchrist, G. K. Brennen, New J. Phys. **11**, 053011 (2010).

[28] R. de-Picciotto, M. Reznikov, M. Heiblum, V. Umansky, G. Bunin, D. Mahalu, Nature **389**, 162 (1997).

[29] F. E. Camino, W. Zhou and V. J. Goldman, Phys. Rev. B **72**, 075342 (2005).

[30] S. Gladchenko, D. Olaya, E. Dupont-Ferrier, B. Doucot, L. B. Ioffe, M. E. Gershenson, Nat. Phys. **5**, 48 - 53 (2009).

[31] J. K. Pachos, W. Wieczorek, C. Schmid, N. Kiesel, R. Pohlner, H. Weinfurter, New J. Phys. **11**, 083010 (2009).

[32] C.-Y. Lu, W.-B. Gao, O. Gühne, X.-Q. Zhou, Z.-B. Chen, J.-W. Pan, Phys. Rev. Lett. **102**, 030502 (2009).

[33] W. Bishara, P. Bonderson, C. Nayak, K. Shtengel, J. K. Slingerland, Phys. Rev. B **80**, 155303 (2009).

[34] A. Y. Kitaev, Proceedings of the 3rd International Conference of Quantum Communication and Measurement, Ed. O. Hirota, A. S. Holevo, and C. M. Caves (New York, Plenum, 1997).

[35] E. Dennis, A. Kitaev, A. Landahl, J. Preskill, J. Math. Phys. **43**, 4452 (2002).

[36] S. Lloyd, Quant. Inf. Proc. **1**, 1 (2002).

[37] C. Mochon, Phys. Rev. A **69**, 032306 (2004).

[38] J. K. Pachos, Int. J. Quant. Inf. **4**, 947 (2006).

[39] S. Bravyi, Phys. Rev. A **73**, 042313 (2006).

[40] L. S. Georgiev, Phys. Rev. B **74**, 235112 (2006).

[41] S. Bravyi and A. Kitaev, Phys. Rev. A **71**, 022316 (2005); S. Bravyi, Phys. Rev. A **73**, 042313 (2006).

[42] R. Raussendorf, J. Harrington, R. Raussendorf, J. Harrington and K. Goyal, Ann. Phys; **321**, 2242 (2006); Phys. Rev. Lett. **98**, 190504 (2007); R. Raussendorf, J. Harrington and K. Goyal, New J. Phys. **9** 199, (2007).

[43] G.K. Brennen, S. Iblisdir, J.K. Pachos, J.K. Slingerland, New J. Phys. **11**, 103023 (2009).

[44] D. Aharonov, V. Jones and Z. Landau, Algorithmica, **55**, 395 (2009).

[45] J. Preskill, http://www.theory.caltech.edu/ preskill/ph219/.

[46] G. Brennen and J. K. Pachos, Proc. R. Soc. London, A **464**, 2089 (2008).

[47] C. Nayak, S. H. Simon, A. Stern, M. H. Freedman and S. Das Sarma, Rev. Mod. Phys. **80**, 3 (2008).

[48] P. Etingof, D. Nikshych and V. Ostrik, math.QA/0203060.

[49] D. Gottesman, Phys. Rev. A **54**, 1862 (1996).

[50] S. S. Bullock and G. K. Brennen, J. Phys. **A40**, 3481-3505 (2007).

[51] A. Kitaev, Ann. Phys. **321**, 2 (2006).

[52] E. Knill, R. Laflamme, and G. J. Milburn, Nature **409**, 46 (2001).

[53] S. Clark, J. Phys. A: Math. Gen. **39**, 2701 (2006).

[54] E. Farhi, J. Goldstone, S. Gutmann, J. Lapan, A. Lundgren, and D. Preda, Science 292, 472 (2001).

[55] V. Lahtinen, G. Kells, A. Carollo, T. Stitt, J. Vala, J. K. Pachos, Ann. Phys, **23**, 9, (2008); V. Lahtinen and J. K. Pachos, New J. Phys. **11**, 093027 (2009).

[56] F. A. Bais, J. K. Slingerland, S. M. Haaker, Phys. Rev. Lett. **102**, 220403 (2009).

[57] V. Lahtinen and J. K. Pachos, arXiv:1003.1086 (2010).

[58] C. Castelnovo and C. Chamon, Phys. Rev. B, **76**, 184442 (2007).

[59] S. Bravyi, M. Hastings and S. Michalakis, arxiv:arXiv:1001.0344v1 (2010).

[60] S. Sachdev, Quantum Phase Transitions, Cambridge: Cambridge University Press, 1999, 8-10.

[61] D. P. DiVincenzo, P. Hayden, B. M. Terhal, Found. Phys. **33**, 1629-1647 (2003)

[62] H, Weimer, M. Müller, I. Lesanovsky, P. Zoller and H. P. Büchler, Nat. Phys. **6**, 382 - 388 (2010).

[63] S. Coleman, Harvard University preprint HUTP-78/A004 (1977).

[64] M. Möttönen, J. J. Vartiainen, and J. P. Pekola, Phys. Rev. Lett. **100**, 177201 (2008).